Patterned Modulation of the Conductivity of Polyaniline Derivatives by Means of Photolithography

MASTER THESIS

by

Simone Viola RADL, BSc

Institute of Chemistry of Polymeric Materials

Thesis Supervisor: Dipl.-Ing. Dr.techn. Thomas Grießer

Academic Advisor: Univ.-Prof. Mag.rer.nat. Dr.techn. Wolfgang Kern

EIDESSTATTLICHE ERKLÄRUNG

Ich erkläre an Eides statt, dass ich diese Arbeit selbständig verfasst, andere als die angegebenen Quellen und Hilfsmittel nicht benutzt und mich auch sonst keiner unerlaubten Hilfsmittel bedient habe.

AFFIDAVIT

I declare in lieu of oath, that I wrote this thesis and performed the associated research myself, using only literature cited in this volume.

_____ _____

Datum Unterschrift

ACKNOWLEDGMENT

I express my gratitude to Dr. Thomas Grießer and Univ.-Prof. Dr. Wolfgang Kern from the Institute of Chemistry of Polymeric Materials (University of Leoben, Austria) for providing me the topic for this Master Thesis, for supervising me and always finding time for helpful advice and scientific instructions.

Furthermore, I thank the colleagues of the working group of Dr. Thomas Grießer for supporting the experimental investigations.

Special thanks are directed to Andreas Pavitschitz from the Institute of Physics (University of Leoben, Austria) for all C-AFM measurements and interpretations.

For GPC measurements I thank Ao. Univ.-Prof. Dr. Nicolai Aust from the Institute of Chemistry of Polymeric Materials (University of Leoben, Austria).

Moreover, I would like to thank Dr. Thomas Rath from the Institute for Chemistry and Technology of Materials (Graz University of Technology) for support with the measurements of the relative sheet conductivity and the realisation of the OLEDs.

But very special thanks are directed to my family and my friends for their support, their patience and their motivating words. In particular, the I would like to thank my mother Susi, my father Hans and Hugo for the financial support und patience during the whole duration of study, sister Marlene and Julia for many weightless sunny days in life and particularly Franz, standing by my side, for giving unflaggingly energy and encouragement.

Abstract

This thesis deals with the synthesis and characterization of photosensitive polyaniline derivatives. Starting from the intrinsically conductive polymers polyaniline and poly-*o*-toluidine the corresponding non-conductive N-formyl derivatives were obtained by means of a formylation reaction.

The illumination of thin films of such polymers with UV-light leads to the decomposition of the N-formyl group resulting in the formation of conductive polymers. This photodecarbonylation reaction was studied using FTIR and UV/VIS spectroscopy. Moreover, thin films of these polymers were patterned by photolithographic methods. Patterned conductive polymer films were obtained by a subsequent doping of the irradiated areas with hydrochloric acid. In addition the irradiated areas became insoluble in organic solvents after protonation. Due to this fact a negative-tone image could be achieved upon the development with dimethylformamide.

The difference in conductivity of these patterned polymer layers were investigated by means of conductive atomic force microscopy (CAFM). Moreover, it turned out that the sheet conductivity of poly-N-formylaniline layers depends on the conversion of the photoreactive groups. In a further step thin films of poly-N-formylaniline were applied as photopatternable hole-transport layer in organic light emitting diodes.

Kurzfassung

Die vorliegende wissenschaftliche Arbeit beschäftigt sich mit der Synthese und Charakterisierung von photoreaktiven Polyanilinderivaten. Aus den beiden intrinsisch leitfähigen Polymere Polyanilin und Poly-*o*-toluidin wurde durch eine Formylierungsreaktion die entsprechenden neuen photoreaktiven, nichtleitenden N-Formyl-Derivate hergestellt.

Eine Belichtung von dünnen Schichten dieser Polymere mit UV-Licht führt zur Abspaltung der Formylgruppe, wodurch wiederum die leitfähigen Ausgangspolymere gebildet werden. Diese Photodecarbonylierungsreaktion der N-Formamidgruppe wurde mit Hilfe von FTIR- und UV/VIS-Spektroskopie untersucht. Weiters konnten dünne Filme dieser Polymere durch photolithographische Methoden strukturiert werden. Durch anschließende Dotierung der belichteten Flächen mit Salzsäure konnten strukturierte leitfähige Polymerfilme erhalten werden. Zusätzlich werden die belichteten Flächen durch die Protonierung in organischen Lösungsmitteln unlöslich. Durch eine anschließende Entwicklung mit Dimethylformamid konnte das entsprechende Negativ Bild erhalten werden.

Der Unterschied der Leitfähigkeit in diesen strukturierten Polymerfilmen wurde mittels Leitfähigkeits-Rasterkaftmikroskopie (CAFM) untersucht. Weiters konnte gezeigt werden dass die Flächenleitfähigkeit von Poly-N-formylanilin Schichten mit dem Umsatz der Photoreaktion zunimmt. In einem weiteren Schritt wurden dünne Filme von Poly-N-formylanilin in organischen Leuchtdioden als photostrukurierbare Lochleiter-Transport-Schicht eingesetzt.

Contents

1 Introduction

In recent years, the synthesis, characterization and modification of the electrically conductive polymers have become one of the most important research areas in science of polymers and materials.[1]

Among conductive polymers, polyaniline (PAn) and its derivatives are of particular interest because of their environmental stability, controllable electrical conductivity, and interesting redox properties which makes them suitable for the application in modern electronic devices.[2,3,4,5] First reports about polyaniline (PAn) can been found in the literature dating back to the late 19th century.[6] Environmetally stable PAn is currently one of the most rapidly growing class of conducting polymers which offer several advantages over metals and find application as polymeric electrodes and interconnects in organic thin film transistors[7,8], organic light emitting diodes[9], batteries[10,11], electrochromic devices[12,13,14] and chemical sensors[15,16].

Electrodes in conventional microelectronic inorganic devices are fabricated using photolithographic techniques, a technique that uses a polymer photoresist chosen for both its sensitivity to radiation and dissolution characteristics, but not for its electronic properties. In macromolecular electronics, the organic material must offer the desirable electronic properties and should also exhibit the possibility for patterning.

The idea of the present work is to synthesise photosensitive polyaniline derivatives bearing pendant N-formamide units which offer the possibility of a patterned modification of the conductivity by means of UV-light.

However, this type of polymer, like many other conductive polymers, is rather insoluble in common organic solvents due to its chain stiffness which causes many limitations with respect to solubility and processability.[17] Soluble derivatives can be synthesised by introducing alkyl groups in the ortho- or meta- positions of the benzyl and quinoidal rings. A well soluble derivative of polyaniline is for example poly-*o*-toluidine (POT) which contains a methyl group in ortho- position.[35]

For that reason the synthesis of a well soluble photosensitive derivative of ortho-toluidine is also intended by introducing N-formyl groups.

2 Theoretical Foundations

2.1 Intrinsically Conductive Polymers

Research into the electronic, optical and magnetical properties of conjugated[i] polymers began in the 1970s after numerous seminal experimental achievements. In the early stages, the synthesis of polyacetylene thin films (Itô et al. 1974) and the subsequent success in doping these polymers to create conducting polymers (Chiang et al. 1977) established the field of synthetic metals.[18]

Typical insulating organic polymers have saturated (sp^3 hybridised) carbons along the backbone of the chain. In organic conjugated polymers, the backbones consist of sp^2 hybridised carbons. This electron configuration results in three σ-bonding electrons, the 2s, $2p_x$ and $2p_y$ electrons and a remaining $2p_z$ electron. Two adjacent $2p_z$ orbitals can overlap, forming a π-bond (see Figure 1). In a conjugated polymer, the $2p_z$ electron orbitals overlap along the backbone, which gives rise to the delocalisation of the π electron system.[19]

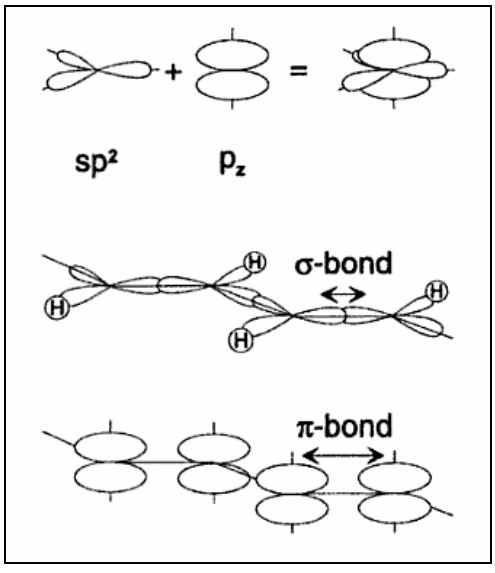

Figure 1: A simple representation of σ-bonds and π-bonds[19]

[i] conjugated (*conjungere,* lat. = to connect): alternating single and multiple (e.g. double) bonds; each atom along the polymer backbone is affiliated to a π bond

An organic polymer that possesses the electrical and optical properties of a metal while retaining the mechanical and processing properties of a conventional polymer, is termed an “intrinsically conducting polymer” (ICP). The properties of these materials are intrinsic to a “doped” form of the polymer.20

The concept of “doping” is the unique, central, underlying, and unifying theme that distinguishes conductive polymers from all other types of polymers. In the doped form the polymer has a conjugated backbone in which the π-system is delocalised. During the doping process, a weakly conducting organic polymer is converted to a polymer which is in the “metallic” conducting regime (up to 10^4 Siemens per centimetre [S/cm]). Increases in conductivity of up to 10 orders of magnitude can be readily obtained by doping. Doped polyacetylene approaches the conductivity of copper on a weight basis at room temperature. Doping is reversible. The original polymer can be recovered with little or no damage to the backbone chain. The doping and undoping processes, involving dopant counter ions that stabilise the doped state, may be carried out chemically or electrochemically. By controlled adjusting the doping level, a conductivity anywhere between that of the undoped (insulating or semiconducting) and that of the fully doped (metallic) form of the polymer may be obtained. All conducting polymers (and most of their derivatives), including polyacetylene, polypyrrole, polythiophene, polyparaphenylene, polyaniline, poly(paraphenylene vinylene), polyfuran, and polyheteroaromatic vinylene (some of them shown in Figure 2), undergo either p- and/or n-redox doping by chemical and/or electrochemical processes during which the number of electrons associated with the polymer backbone changes. P-doping involves partial oxidation of the π-system, whereas n-doping involves partial reduction of the π-system. Polyaniline, the best known and most fully investigated example, also undergoes doping by a large number of protonic acids, during which the number of electrons associated with the polymer backbone remains unchanged.[20]

Appropriate forms and derivatives of many conducting polymers, especially those involving polyaniline and polythiophene, are readily solution processible into freestanding films or can be spun into fibres that even at this relatively early stage of development have tensile strengths approaching those of the aliphatic polyamides.[20]

The thermal, hydrolytic, and oxidative stability of doped forms of pure conducting polymers varies enormously from the n-doped form of polyacetylene, which undergoes instant decomposition in air, to polyaniline, which has sufficient stability in air at 240°C to permit blending and processing with conventional polymers. The oxidative and hydrolytic stability is significantly increased when the conducting polymer is used in form of blends with conventional polymers. Clearly, research to improve the stability of conducting polymers is essential to commercial applications in future.[20]

Polyaniline is currently the leading conducting polymer used in technological applications and is commercially available in quantity. Polypyrrole and derivatives of polythiophene and poly(paraphenylen vinylene) also have significant potential technological applications. Rechargeable polyaniline batteries and high-capacity polypyrrole capacitors are in commercial production.[20]

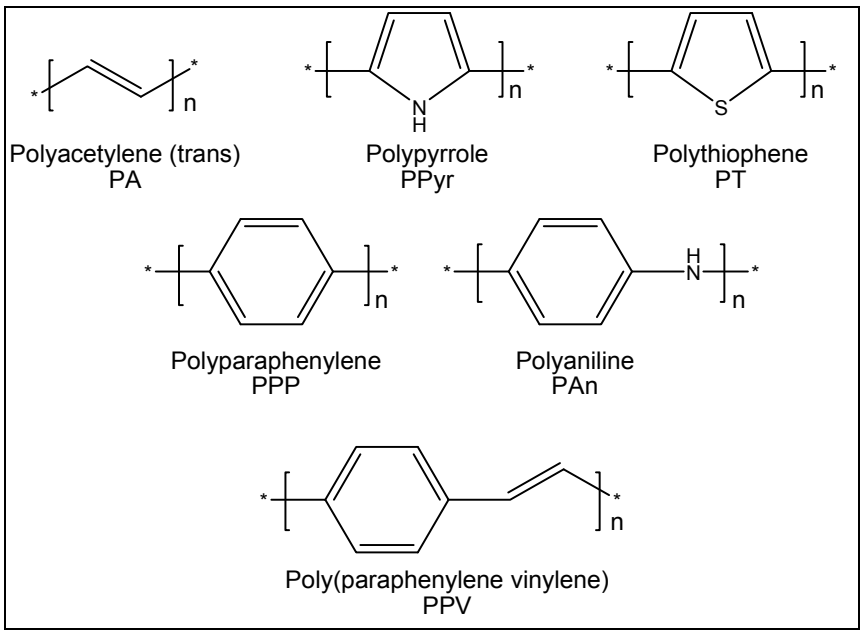

Figure 2: Structures of some conjugated polymers and their common abbreviation

2.1.1 Polyaniline (PAn)

Polyaniline may be the oldest synthesised polymer and is of great scientific and industrial interest for research and technological applications in electrical devices.[21]

For the first time the monomer aniline was received from the pyrolytic distillation of indigo and was called “Krystallin” because it generated well formed crystalline salts in sulfuric and phosphoric acidic media. In 1840, Fritzsche also obtained a colorless oil from indigo and oxidized it to polyaniline (PAn). Some believe this to be the first report of polyaniline, although the first definitive report of polyaniline did not occur until 1862.[6]

For the following about hundred years polyanilines just rarely took part in science until the studies by MacDiarmid et al. in the mid 1980s.[22,23] The sensational discovery of the electrical conductivity of emeraldine salt took polyaniline to a great scientific and industrial interest, till nowadays.

2.1.1.1 Synthesis and Structure

Synthesis of Polyaniline

In general polyanilines are prepared through chemical and electrochemical oxidative polymerisation in acidic solution. Polyaniline exhibits predominantly head-to-tail polymerisation with essentially linear chains. A wide range of polymerisation techniques[24] have been found, including:

- Electrochemical polymerisation
- Chemical polymerisation
- Photochemically initiated polymerisation
- Enzyme-catalysed polymerisation
- Polymerisation employing electron acceptors

Molecular Structure

Chain Structure and Oxidation Forms

The general polymeric structure of PAn is shown in Figure 2 below. The polymer forms linear chains and in solution either tight coils or expanded chains appear, depending on the used solvent.

Polyaniline can exist as base or salt in three readily accessible oxidation steps. The fully reduced colorless polybenzenoid leucoemeraldine (LES, LEB) is insulating. The partially oxidized blue emeraldine base form (EB) can become conductive in acidic media (emeraldine salt, ES, in green) and then exhibits maximum conductivity. Further oxidation finally leads to the insulating blue-black polyquinoid pernigraniline form (PB, PS).[21,24,25]

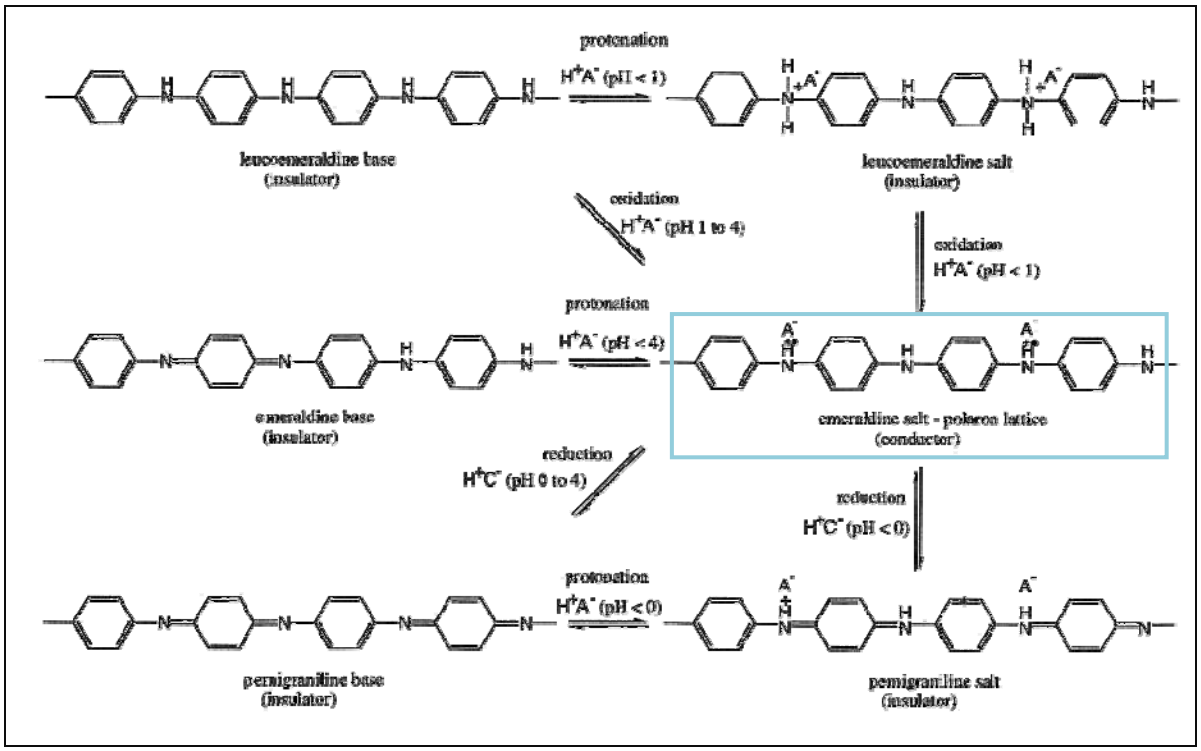

Figure 3: Various oxidation states in base or salt form[26]

As shown in Figure 3 the protonated form associates counter-anions with the positively charged polyaniline chains. All these forms constitute PAn as a complicate structure by its complexity.

Molecular Weight

Mattes et al.[27] had explored the correlation between polymerisation temperature and molecular weight. According to them the molecular weights (M_W) nearly increased tenfold as the polymerisation temperature decreased from 0°C to -40°C (using GPC with polystyrene standards and LiCl as solvent to prevent PAn H-bonding interactions). The higher the molecular weight, the better films could be cast and the higher was the tensile strength.

Bulk Structure[28]

There is considerable evidence and widespread acceptance that PAn forms a heterogeneous structure in its emeraldine salt form. It is proposed that small domains of highly ordered polymer are surrounded by less ordered material and that electron transport is

dominated by slow conduction through the latter. In the ordered regions, it is suggested that the polymer chains lie flat, allowing a longer conjugation length as the π orbitals can overlap. In the amorphous regions, the chains are more twisted, causing less overlap of π orbitals and shorter conjugation lengths.

Preparation conditions determine whether the emeraldine salt or base is either amorphous or crystalline. There are some differences in the crystallographic structure after protonation, deprotonation and re-protonation again:

- ES-I structure: Direct polymerisation of aniline in acidic media produces the doped PAn-form emeraldine salt (ES).
- EB-I structure: The amorphous emeraldine base (EB) results after deprotonation of ES and re-protonation leads to the ES-I again.
- EB-II structure: A new crystallographic structure is generated by dissolving EB-I in several solvents and casting as a film. EB-II is crystalline with a crystallinity of about 50 %.
- ES-II structure: Doping of EB-II with acid leads to the ES-II structure, again with a crystalline percentage of 50 %, and is significantly different to the ES-I. Deprotonation produces curiously an amorphous EB, and re-protonation the ES-II again.

2.1.1.2 Properties and Postpolymerisation Modification

Electrical properties

As described above, electrical conductivity depends not only on the oxidation level but also on the doping degree of PAn. Maximum conductivity can be reached after doping the emeraldine form.

There are several different possibilities to dope the emeraldine form: with agents such as Brönsted acids (HA), Lewis acids and metal complexes, or organic electron acceptors.

In the focus of this work is the doping with Brönsted acids such as the inorganic acids HCl, HNO_3, H_2SO_4, H_3PO_4, HBF_4, and organic sulfonic and carboxylic acids.

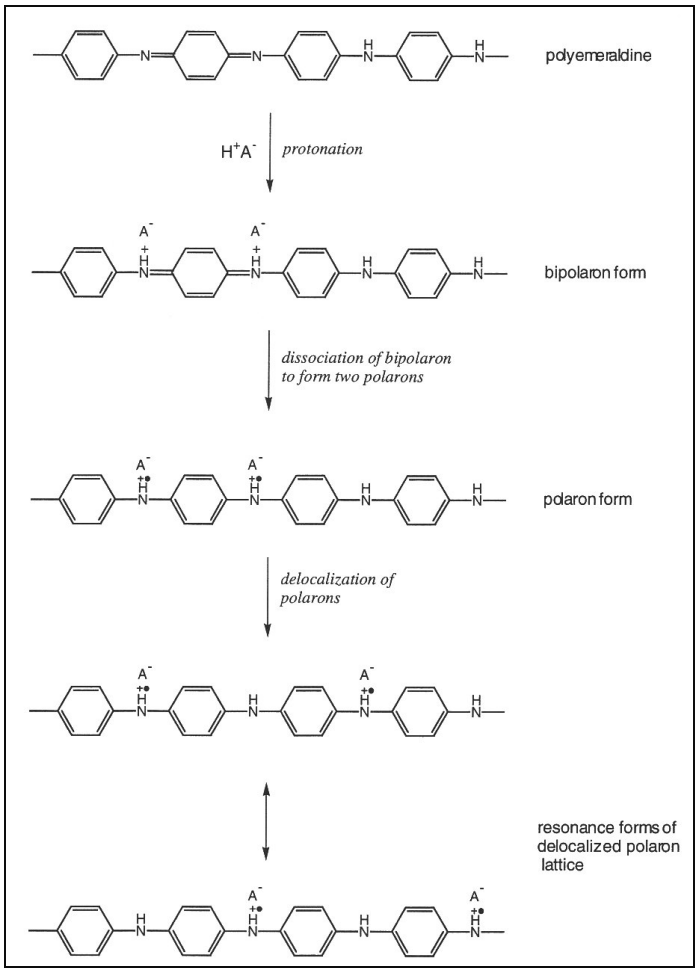

Figure 4: Protonation process in detail[26]

As already mentioned, the oxidation state, that can be doped to give the highly conducting state, is polyemeraldine. It consists of amine (-NH-) and imine (=N-) sequences in equal proportions. The imine sequences are protonated by acids to the bipolaron (dication salt) form. A further rearrangement leads to the delocalized polaron lattice (polysemiquinone radical-cation salt). These different process steps are shown in Figure 4.[17,26]

The bipolaron form is much more energy efficient than the polaron form according to theoretical calculations,[29] but really high conductivity due to polarons as additional charge carriers. Further there is a wide range of influences on the conductivity such as temperature, humidity (polymer water content), structural defects and polymer morphology, and also the solvent the polymer is cast from.[17,26]

The maximum conductivity is reached if PAn is doped 50 % as the polarons lattice show in Figure 4.The overlapping polarons form mid-gap bands. Conduction is permitted when the electrons are thermally brought up to the lower energy unfilled bands at ambient temperatures. This model can be compared with semiconductive materials. At higher doping

levels also amine sequences will be protonated, at lower levels imine sequences will remain unprotonated. In both cases an interruption of delocalisation of the charge carriers and less conductivity are the consequences.[17,26,30]

Mechanical properties

Solubility

Polyaniline emeraldine form exists as a dark blue powder which is difficult to process because of its lack of solubility. This results from the stiffness of polymer backbone and the hydrogen-bonding between adjacent polymeric chains.[21]

In general PAn is moderately soluble in polar organic solvents such as *N,N*-dimethylformamide (DMF), dimethyl sulfoxide (DMSO), and *N*-methylpyrrolidone (NMP). The solubility of the base form is much better than that of the salt form.[31,35]

To control solubility it is possible to modify the polymeric chain by introducing alkyl [17,32] or alkoxyl[33] substituents.

2.1.2 Poly-*o*-toluidine (POT)

Poly-*o*-toluidine is a chemically modified form of PAn where the ortho position of the benzyl and quinoid ring contains a methyl group instead of a hydrogen atom (see Figure 5).

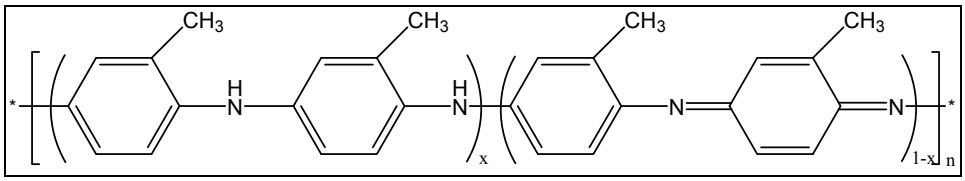

Figure 5: Structure of poly-*o*-toluidine

POT is known to be soluble in many common organic solvents and so it is much easier to process and characterise than PAn.[34]

It is reported that, after chemical or electrochemical copolymerisation of aniline with *o*-toluidine, POT also shows interesting electrochemical properties because of a reduction in π-conjugation caused by steric effects of the methyl groups.[32]

The processes, more precisely the oxidation steps and doping processes, stay the same as in case of PAn because these processes all refer to the amine and imine units.

3 Current State of Art and Definition of Task

In the literature several approaches for direct photolithographic patterning of PAn have been reported. Most of them refer to the photo-doping of thin PAn films by means of photo acid generators.[35] The photogenerated acid groups in the irradiated regions protonate the PAn and as a result of this, electrical conductivities up to 0.1 S cm^{-1} for PAG concentrations ranging from 10 to 50 mol % could be obtained. Moreover, doped PAn is typically insoluble in organic solvents in contrast to pristine PAn which offers the possibility of direct photo patterning. Furthermore, electron-beam irradiation is also effective in doping PAn/PAG composite films.[36] Another approach is to cast PAn in its protonated, conductive form in the presence of an aliphatic phenylketone.[37] Upon exposure the ketone generates radicals that reduce PAn to its non-conductive leucoemeraldine form. The unexposed regions have a sheet resistance of 1 kΩ/square after the removal of the photoinitiator by postbaking. The resistance of the exposed region increases dramatically from 1 kΩ/square to 10^{14} Ω/square. This method has been applied for the fabrication of electrodes and interconnects in all polymer OTFTs.[38]

Another possibility for the realization of patterned PAn films is the derivatization of the secondary amino groups using acid labile protective groups. For example, a tert-butyloxycarbonyl (t-BOC) substituted PAn blended with photo acid generators can be patterned by means of photolithography.[39] Illumination with UV-light decomposes the PAG and consequently acid is formed which cleaves the t-BOC group converting the PAn into its conductive and insoluble emeraldine salt form after postbaking at 110°C. Subsequently, the unexposed regions can be removed by washing with chloroform to generate negative tone conductive patterned PAn films providing an electrical conductivity of about 10^{-3} S/cm.

Moreover, conductive patterns of PAn have also been prepared by radiation induced crosslinking.[40] However, all these methods require photosensitive polymer additives for the patterning process and furthermore the obtained polyaniline layers do not reach the conductivity of pristine doped polyaniline which offers values of 3-5 S/cm.

This work aims at the synthesis and characterization of photosensitive polyaniline derivatives bearing pendant N-formamide units which offer the possibility of a patterned modification of the conductivity by means of UV light. An illumination with UV light leads to a decarbonylation reaction of the pedant N-formamide groups resulting in polyaniline and carbonmonoxide.

The formamide unit is a well known photo protective group for aromatic primary amino groups in low molecular compounds.[41] However, the irradiation of polymers bearing

secondary formamides leads to the formation of hydrazobenzene and azobenzene along with other products which cause a cross-linking making such materials suitable for an application as photoresist.[42] Recently, we have reported on the photodecarbonylation of tertiary N-formamides groups in poly(2-vinyl-9H-cabazole-9-carbaldehyd) with respect to a patterned modification of the refractive index.[43] In contrast to secondary amides, the photoreaction of tertiary amides results in less reactive secondary amino groups and therefore no consecutive reactions are expected.

In course of this thesis the photoreaction was investigated by means of UV/VIS and FTIR spectroscopy. Moreover, thin films of such polymers were patterned using photolithographic methods. The obtained patterned films were investigated with respect to changes in conductivity and solubility.

Finally, these photosensitive polymeric films can find application as photopatternable hole transport layers in organic light emitting diodes (OLEDs) in order to realize photostructured devices.

4 Results and Discussion

4.1 Synthesis of the Polymers

In the course of this work poly-*o*-toluidine in two different oxidation forms i.e. the leucoemeraldine form (POT-e) and emeraldine base form (POT-l) have been synthesized. In a subsequent step both polymers were converted into their N-formyl derivatives using a mixture of acetic anhydride and formic acid as formylation agent. Moreover, poly-N-formylaniline (FPAn-e) was synthesized by a fomylation reaction of polyaniline in its emeraldine form.

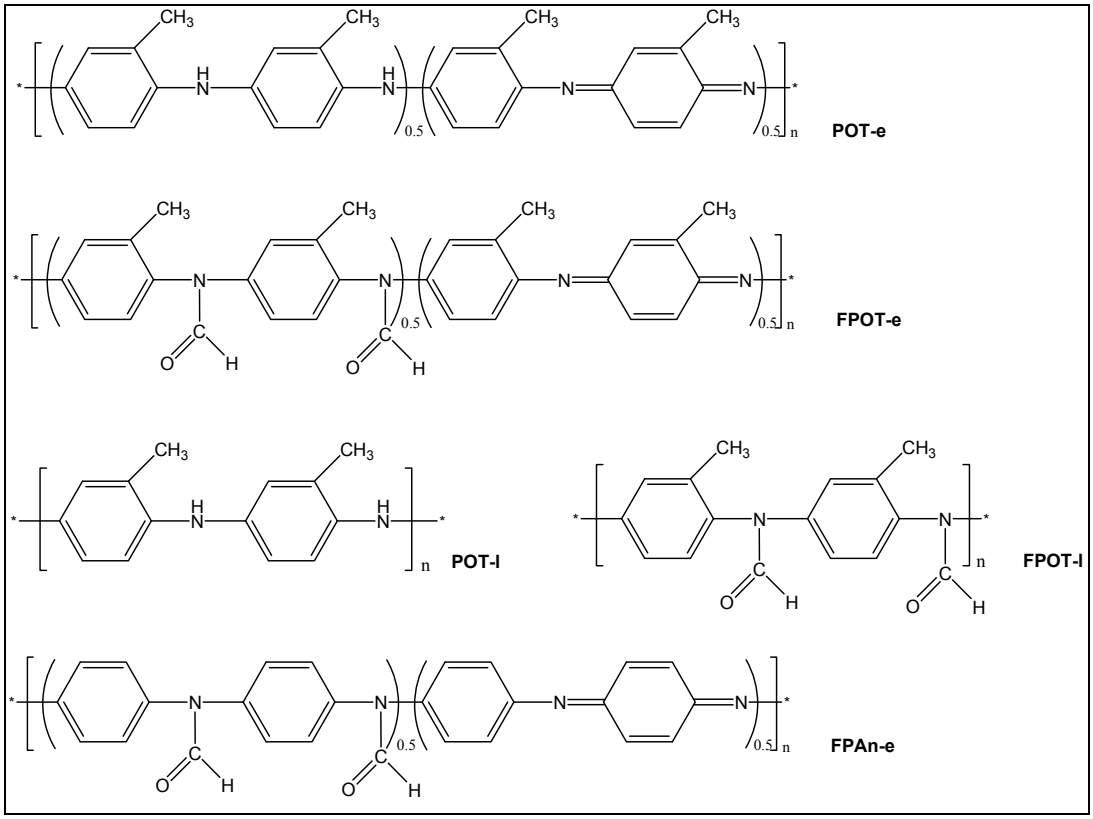

Figure 6: Synthesised polymers

The measured spectroscopic data are in accordance with the proposed chemical structure of the polymers (see Figure 6).

4.1.1 Poly-*o*-toluidine (emeraldine base)

POT-e was synthesised by an oxidation reaction of *o*-toluidine using ammonium persulfate as shown in Figure 7. As a catalyst ferrous sulphate was used. After adding ammonium persulfate POT in the emeraldine salt form i.e. conductive form could be obtained. In a subsequent step ammonium hydroxide was used in order to convert the salt to the emeraldine base form.[35]

The whole synthesis (see Figure 7) of POT-e proceeded smoothly and a yield of about 34 % could be achieved. The obtained POT-e is a deep blue, nearly black powder which shows excellent solubility in THF.

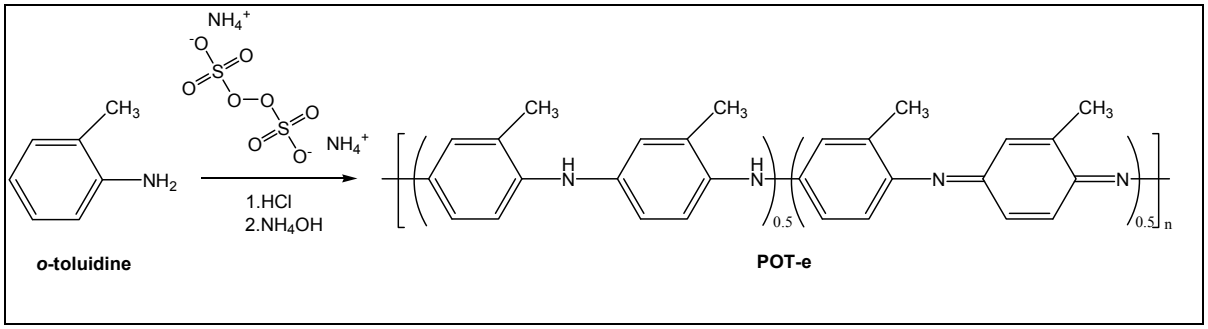

Figure 7: Synthesis of POT-e

The polymer POT-e shows excellent film forming properties when spin cast from dichloromethane solutions leading to fully transparent films with optical quality.

Figure 8 shows the FTIR spectrum of a thin film of POT-e. The peak at 3380 cm^{-1} is typical for the NH- vibration of the secondary amino groups. Moreover, the peak at 1650 cm^{-1} can be attributed to the C=N vibration of the quinoid ring.

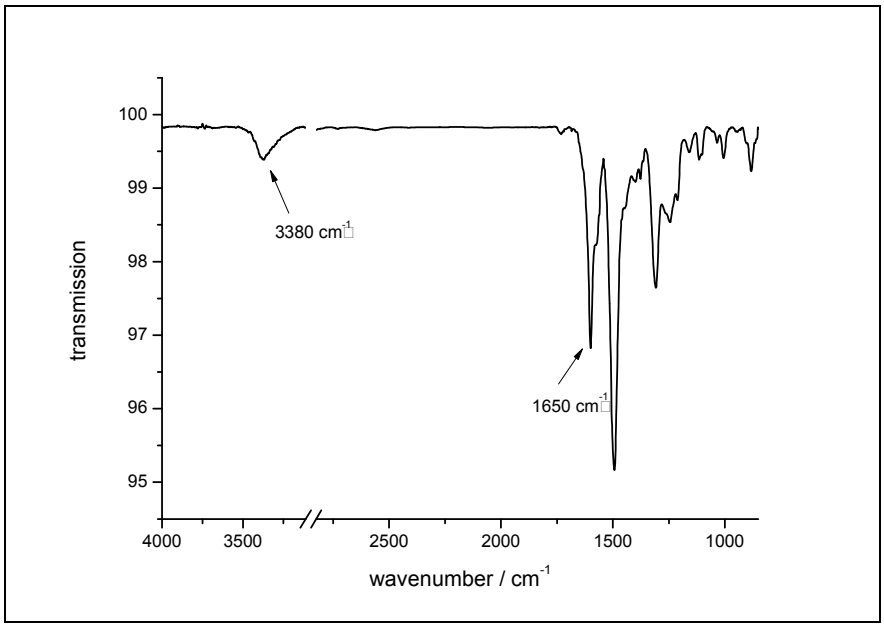

Figure 8: FTIR spectrum of a thin film of POT-e

The ^{1}H-NMR of POT-e (measured in $CDCl_3$, Figure 9) also shows the expected signals for this polymeric material. The signal at 1.92-2.43 ppm can be assigned to the hydrogen atoms of the methyl groups. At around 7 ppm the signal of the hydrogen atoms of the secondary aminogroups can be detected whilst the aromatic hydrogen atoms appear in the range of 6.4-7.5. In addition, the integrals of the signals are in good accordance with the theoretical expectations.

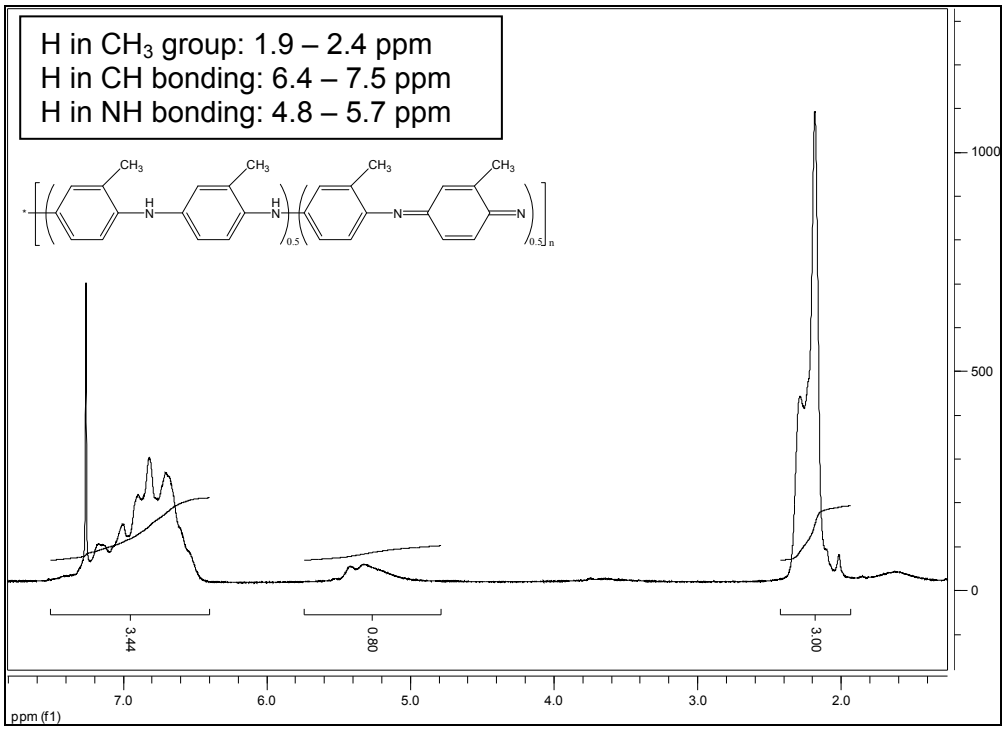

Figure 9: NMR spectrum of POT-e

4.1.2 Poly-N-formyl-*o*-toluidine (emeraldine base)

Poly-N-formyl-*o*-toluidine (FPOT-e) is easily accessible by a polymer-analogous reaction as shown in Figure 10.

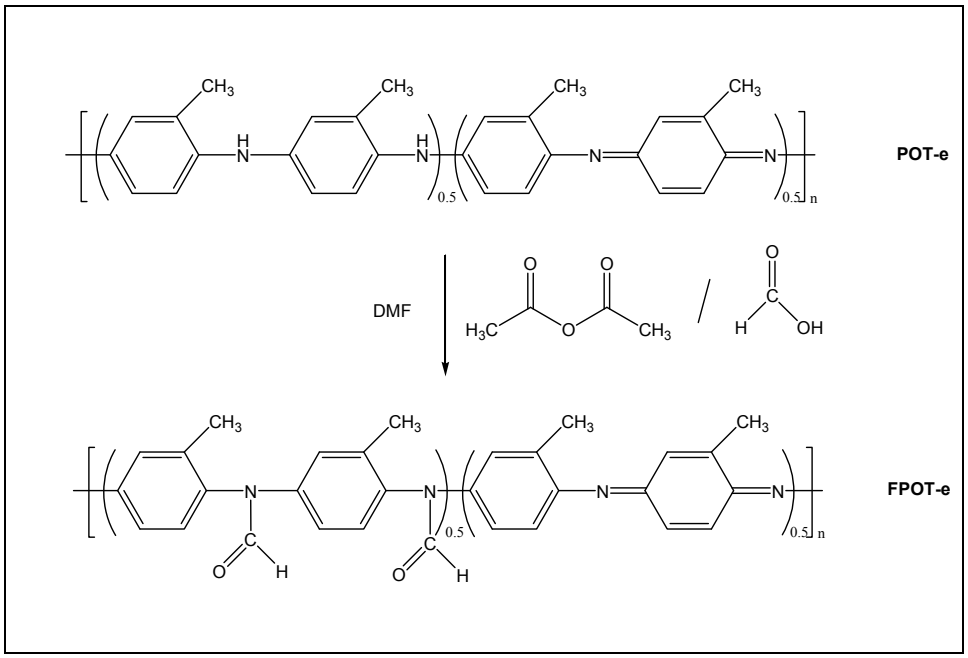

Figure 10: Synthesis of FPOT-e

The preparation of FPOT-e was performed using a mixture of acetic anhydride and formic acid as formylation agent and POT-e as starting material. FPOT-e was obtained after precipitation in diluted ammonia solution.

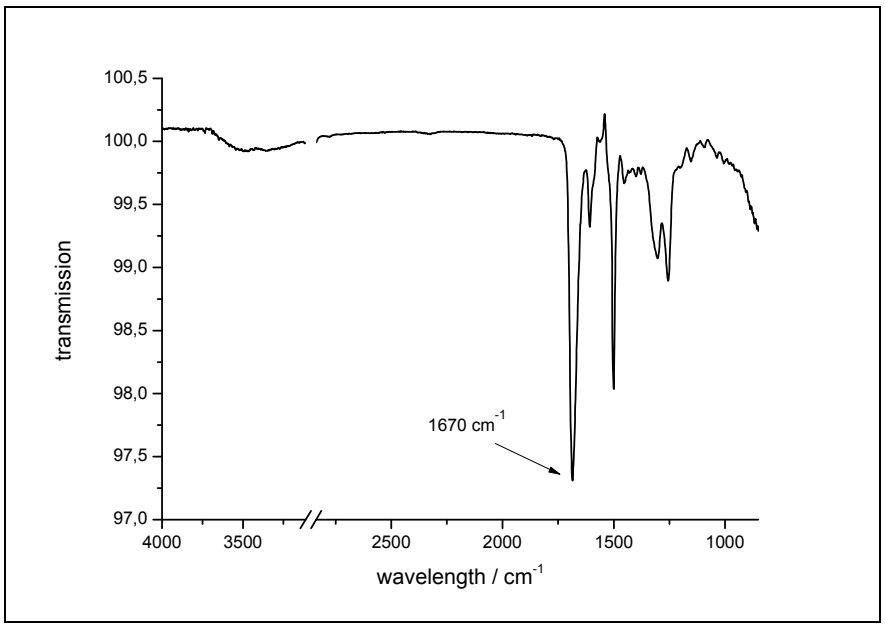

Figure 11: FTIR spectrum of a thin film of FPOT-e

Figure 11 shows the FTIR-spectrum of a thin film of FPOT-e. In contrast to POT-e (Figure 8) a new peak at 1670 cm^{-1} can be observed. This peak can be attributed to the C=O stretching vibration of the N-formyl group. In addition the NH peak at 3380 cm^{-1} has decreased in intensity.

4.1.3 Poly-*o*-toluidine (leucoemeraldine base)

Starting from POT-e the leucoemeraldine base could be obtained by a simple reduction reaction using *N,N*-diethylhydroxylamine as described in the literature (see Figure 12).[44]

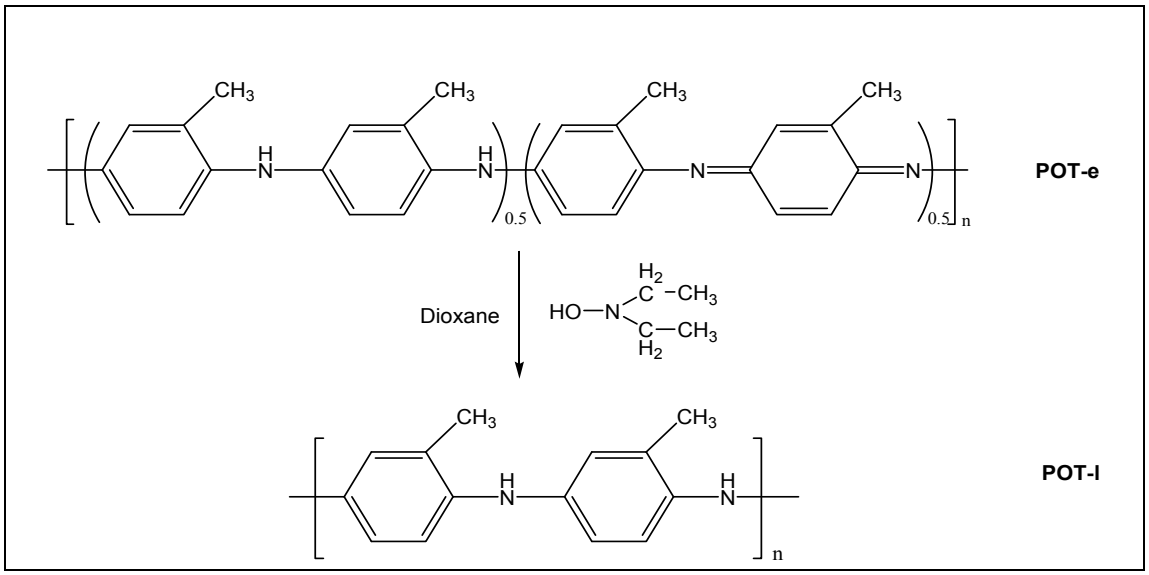

Figure 12: Synthesis of POT-l

During the reaction the colour of the solution changed, as expected, from dark blue to light yellow and finally the solution became nearly colourless.
However, after evaporation of the solvent (dioxane) the colour of the residue changed back to light blue. This fact can be explained by a partial oxidation of the POT-l by atmospheric oxygen. Nevertheless, the FTIR spectrum of POT-l in Figure 13 shows in contrast to the spectrum of POT-e (Figure 8) a less distinctive C=N peak at 1650 cm^{-1} which indicates a partial reduction of the quinoid ring.

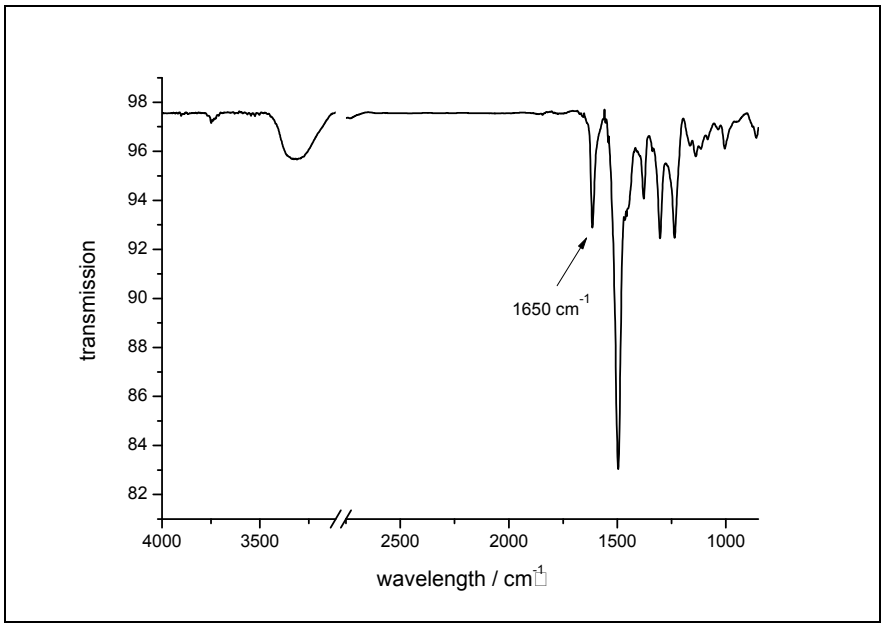

Figure 13: FTIR spectrum of a thin film of POT-I

4.1.4 Poly-N-formyl-*o*-toluidine (leucoemeraldine base)

The preparation of FPOT-I was also performed using a mixture of acetic anhydride and formic acid as formylation agent and POT-I as starting material. (see Figure 14).

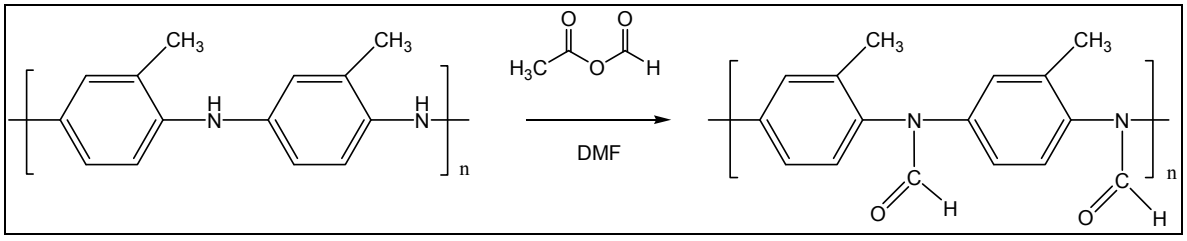

Figure 14: Formylation of FPOT-I

Figure 15 shows the FTIR spectrum of a thin film of FPOT-I. This spectrum is dominated by the strong C=O peak of the formamide group at 1670 cm^{-1}. Nevertheless, the C=N vibration at 1650 cm^{-1} exhibits a similar intensity as the C=N peak in the spectrum of the FPOT-e (Figure 11). This fact can be attributed to a further oxidation of the POT-e during the formylation reaction. For that reason it can be assumed that in this reaction mainly FPOT-e was obtained.

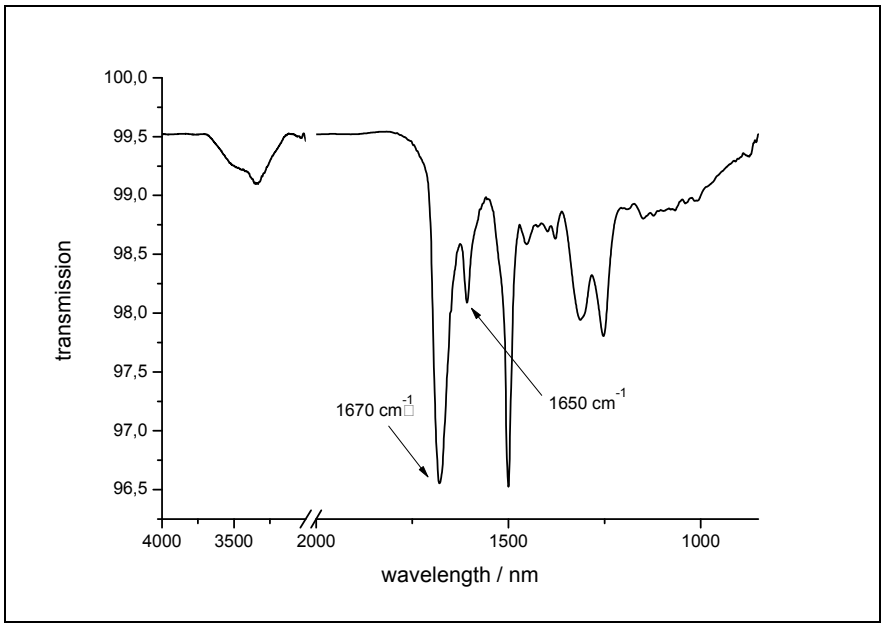

Figure 15: FTIR spectrum of a thin film of FPOT-I

4.1.5 Poly-N-formyl-aniline (emeraldine base)

The photoreactive polyaniline derivative poly-N-formylaniline (FPAn-e) is also accessible by a polymer-analogous reaction as shown in Figure 16. The synthesis of FPAn-e was performed in dimethyformamide (DMF) using a mixture of acetic anhydride and formic acid as formylation agent and the emeraldine base of polyaniline (PAn-e, purchased from Aldrich) as starting material.

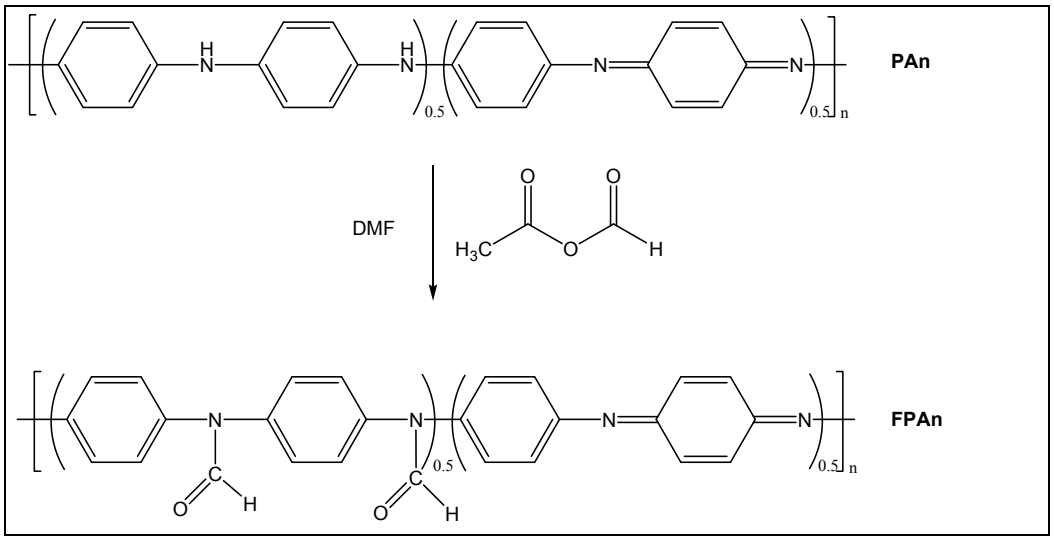

Figure 16: Synthesis of FPAn-e

The FTIR spectrum in Figure 17 shows also a new peak at 1670 cm-1 which indicates the C=O vibration.

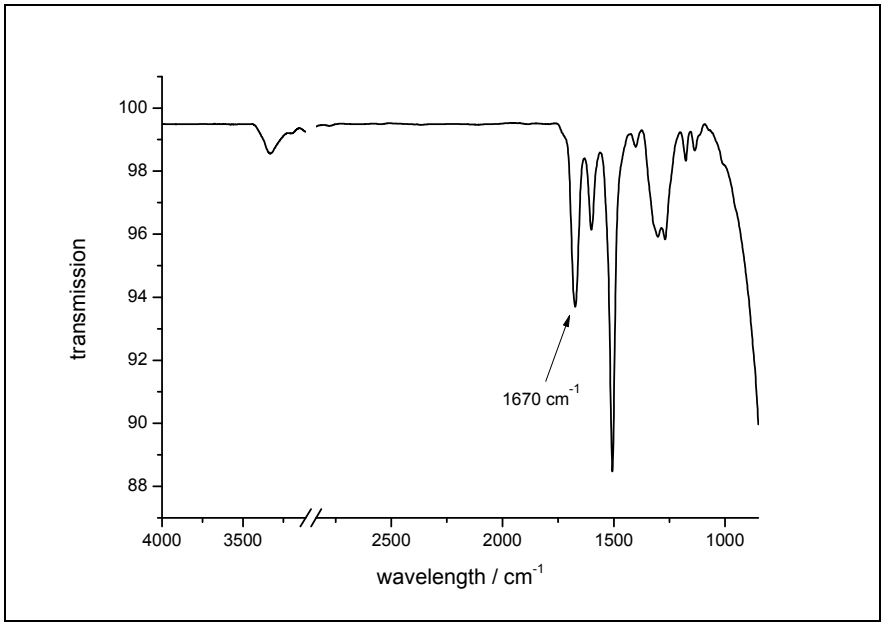

Figure 17: FTIR spectrum of a thin film of FPAn-e

4.2 Investigation of the Photo-Decarbonylation Reaction by Means of UV/VIS and FTIR Spectroscopy

Upon irradiation with UV light the N-formamide groups in the investigated polymers undergo a photodecarbonylation reaction leading to the corresponding polyaniline derivative. Figure 18 displays this photoreaction in the different polymers. Because of this significant change in the chemical structure of the polymers, the photoreaction can be easily followed by spectroscopic methods such as UV-VIS and FTIR spectroscopy.

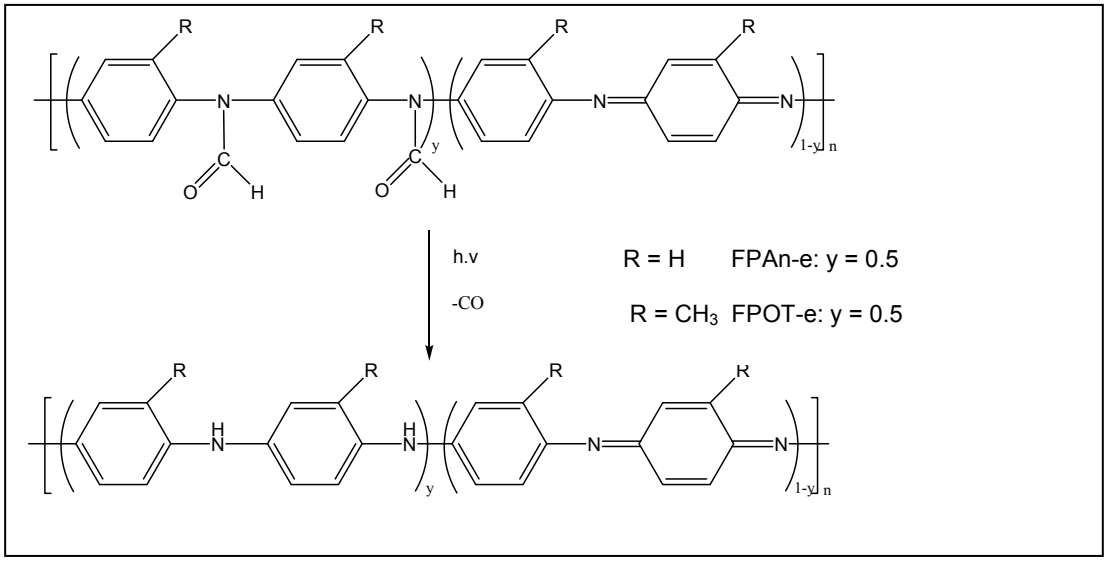

Figure 18: Decarbonylation reaction in the investigated polymers.

4.2.1 Investigation of the Photoreaction of Poly-N-formyl-o-toluidine (emeraldine base)

Figure 19 shows the UV absorbance spectra of a thin film of FPOT-e before and after illumination with UV-light (260-320 nm, P = 270 J/cm^2). The UV/VIS spectrum of the unilluminated polymer film is dominated by a strong maximum at 267 nm. This peak can be attributed to the tertiary N-formamide moieties in the polymer. An illumination with UV-light (260-320 nm) leads to a significant decrease of this maximum (see Figure 19), while a new absorption maximum at 315 nm evolves which can be assigned to a π-π* transition of the photogenerated POT-e.[35] However, in comparison to the UV-spectrum of POT-e which is described in literature, the absorption maximum at 600 nm (assigned to an intermolecular

and/or intermolecular charge transfer process from the benzenoid to the quinoid ring) cannot be found in the spectrum of the photogenerated polymer.[35]

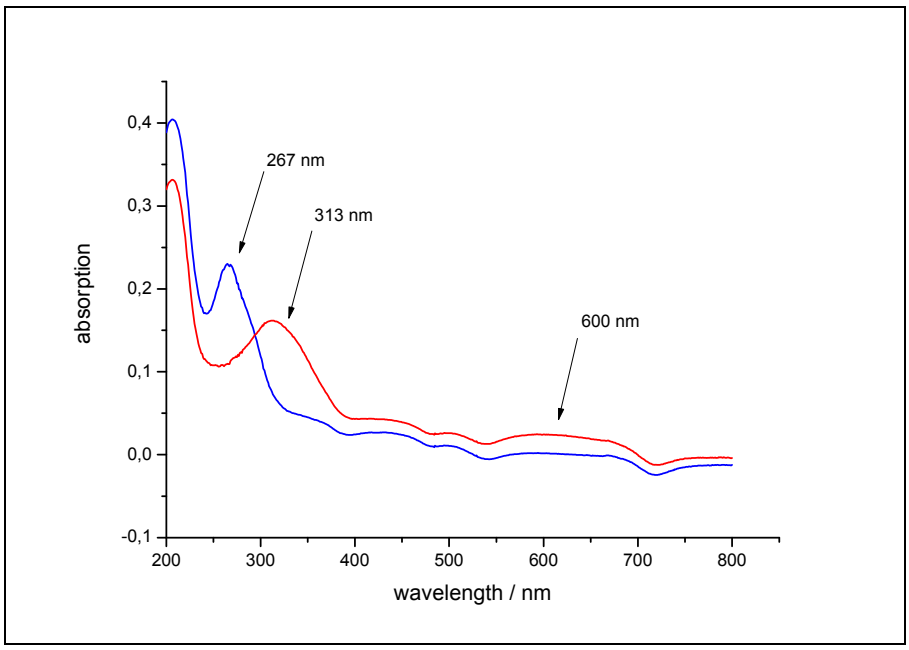

Figure 19: UV/Vis spectra of a thin film of POT-e before (blue line) and after UV irradiation (red line) (medium pressure mercury lamp, λ= 260-320 nm, P = 270 J/cm^2)

Moreover, the FTIR spectrum of the polymer changes upon illumination. Figure 20 shows detailed FTIR spectra of a thin film of FPOT-e before (a) and after illumination (b) with UV light (260-320 nm, P = 270 J/cm^2). In the spectrum of the non-irradiated film the signal at 1670 cm^{-1} (C=O stretch) is typical of N-formamides. After UV irradiation, the vibration band at 1670 cm^{-1} has almost disappeared. Instead, a new peak at 3380 cm^{-1} evolves which arises from the N-H stretching vibration of the formed secondary amino groups.

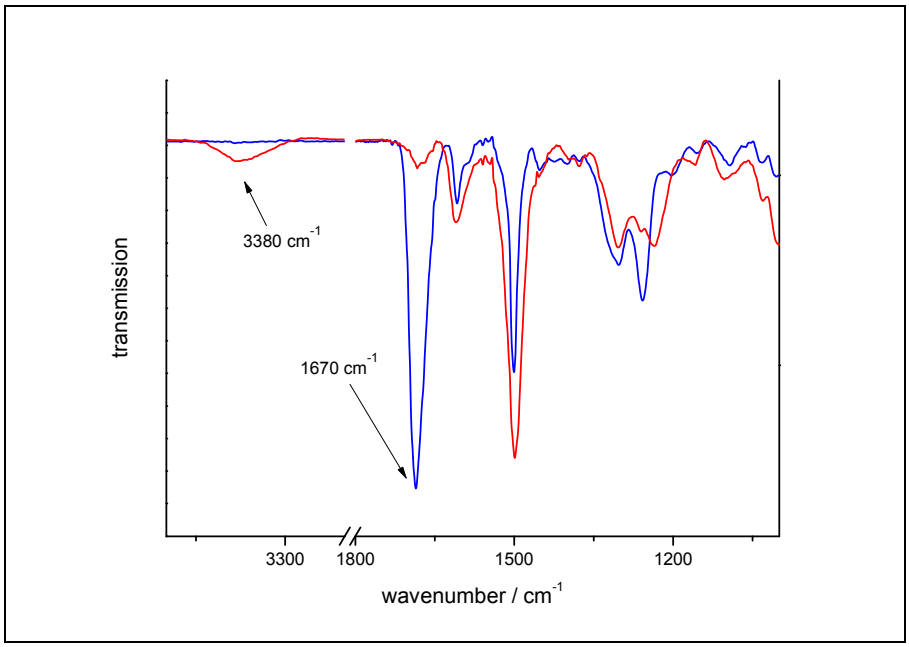

Figure 20: FTIR spectra of a thin film of POT-e before (blue line) and after (red line) irradiation (medium pressure mercury lamp, λ= 260-320 nm, P = 270 J/cm^2)

A kinetic study (Figure 21) of the photo reaction was carried out using the C=O vibration peak of the formamide group at 1670 cm^{-1}. For that reason thin films of FPOT-e were illuminated for defined periods, and absorbance FTIR spectra were recorded. The depletion of the formamide signal was quantified by a tangent fit. The disappearance of the formamide group follows a first order kinetics. After two minutes of illumination already 50 % of the formamide group have been converted. The conversion takes 15 minutes of UV irradiation. At this point the conversion of the formamide group is approximately 90 %.

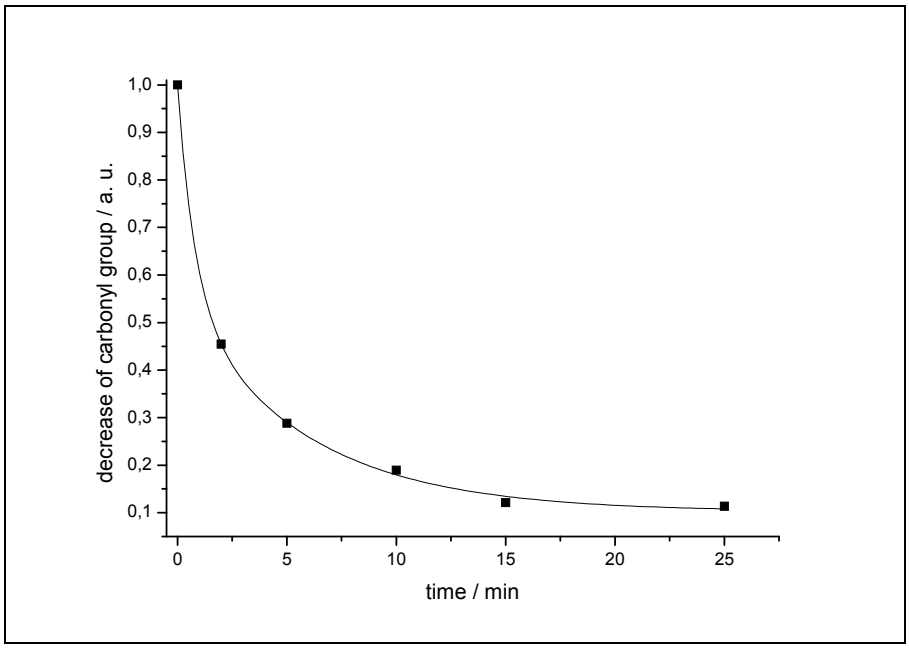

Figure 21: Kinetic study of the decarbonylation of POT-e during irradiation with UV-light (medium pressure mercury lamp, λ= 260-320 nm, E = 180 mW/cm^2). The fitted curve serves as guide to the eye.

However, it can be deduced from the UV/VIS spectrum that the photoreaction does not lead to POT in its emeraldine form. Moreover, a treatment with gaseous hydrochloric acid does not result in the expected change in the UV/VIS absorption as described for pristine POT-e.[35]

Therefore, the approach of photosensitive FPOT-e was not continued in this work.

4.2.2 Investigation of the Photoreaction of Poly-N-formylaniline (emeraldine base)

Figure 23 shows the detailed FTIR spectra of a film of FPAn-e before (a) and after illumination (b) with UV light (270-353 nm, mask aligner, 122.1 J/cm^2). In the spectrum of the non-irradiated film the signal at 1670 cm^{-1} (C=O stretch) is typical of N-formamides. After UV irradiation, the vibration band at 1670 cm^{-1} has almost disappeared. Instead, a new peak at 3380 cm^{-1} evolves which arises from the N-H stretching vibration of the formed secondary amino groups.

The comparison of the FTIR spectrum of FPAn-e after irradiation (Figure 23) with the FTIR spectrum of pristine polyaniline (Figure 22) reveals that these spectra are almost identical. Only, the N-H stretching vibration at 3380 cm^{-1} in the illuminated spectrum of FPAn-e is not that pronounced as in the spectrum of pristine PAn-e.

From this it was concluded that mainly polyaniline is generated by photoextrusion of CO and that side products are formed only to a low extent. Consequenty, the depletion of the carbonyl band directly corresponds to the yield of polyaniline as the photodecarbonylation product.

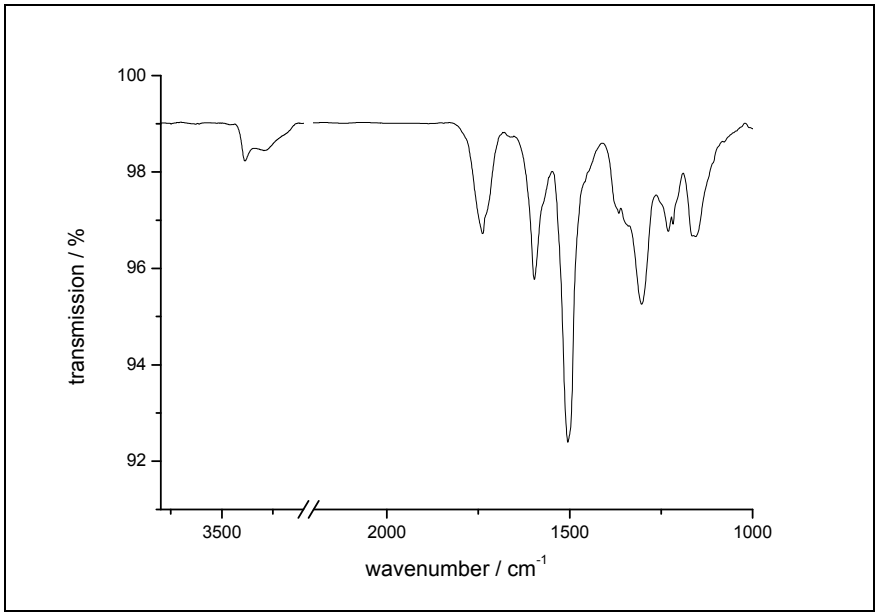

Figure 22: FTIR spectrum of a thin film of pristine PAn-e

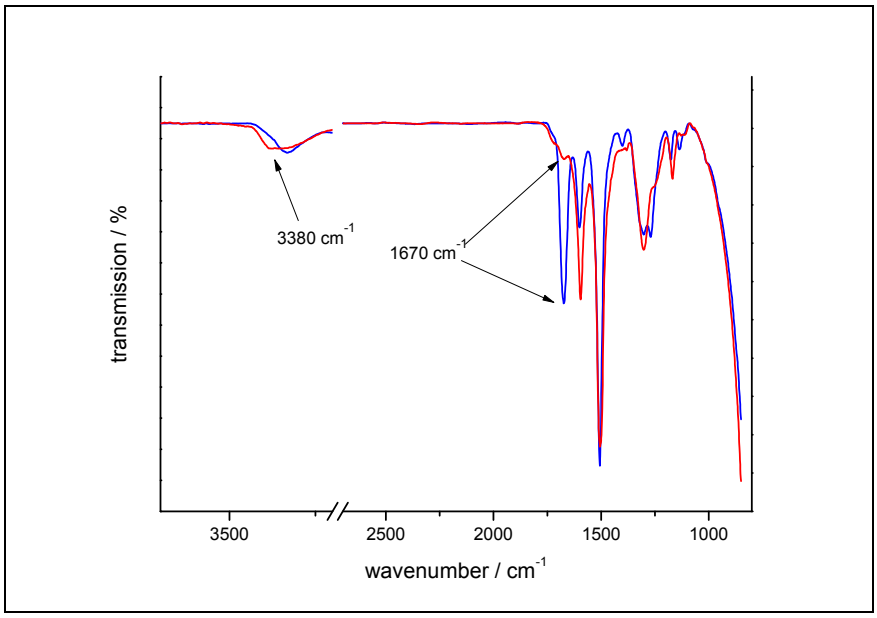

Figure 23: FTIR spectra of a thin film of FPAn-e before (blue line) and after UV irradiation (red line) (mask aligner, 122.1 J/cm^2, λ= 270-353 nm)

Moreover, the UV absorbance spectra of the polymer changes upon illumination. As shown in Figure 25 (blue line), the UV/VIS spectrum of FPAn-e is dominated by a strong maximum at 310 nm. This peak can be attributed to the tertiary N-formamide moieties in the polymer. The illumination with UV light (270-353 nm, mask aligner, 122.1 J/cm^2) leads to a significant decrease of this maximum (see Figure 25, red line). Concomitantly, a new absorption maximum at 630 nm evolves upon irradiation which indicates the formation of PAn-e. The UV spectrum upon irradiation is comparable to that found for pristine polyaniline emeraldine base as shown in Figure 24.

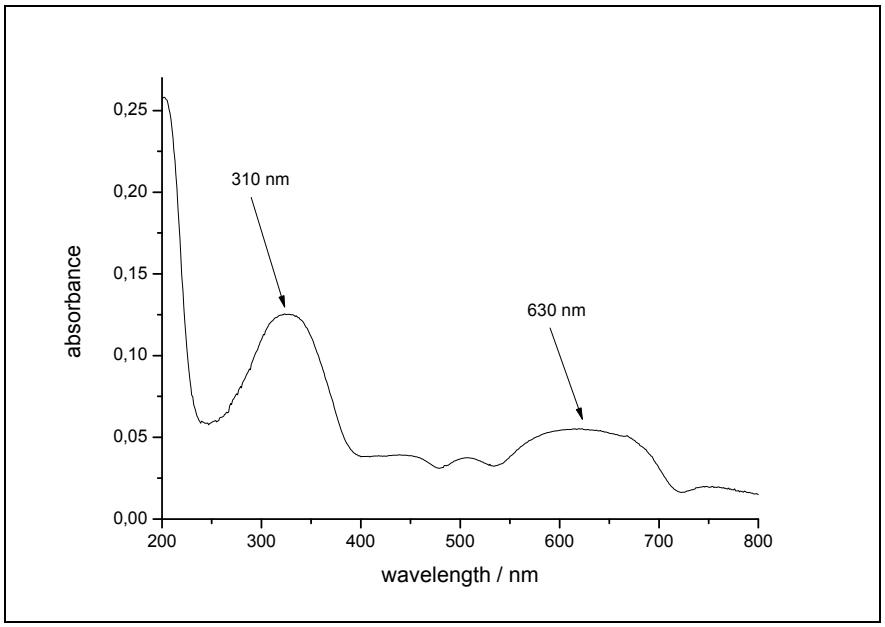

Figure 24: UV/VIS spectrum of a thin film of pristine PAn (emeraldine base).

The band with a maximum of 630 nm is assigned to an intermolecular and/or intramolecular charge-transfer process from the benzenoid to the quinoid ring, leading to the formation of a molecular excitation.[45] The absorption band at around 310 nm which remains upon UV irradiation is due to a π-π* transition.[46]

An exposure of the UV illuminated FPAn-e to gaseous hydrochloric acid leads to changes in the UV absorbance spectrum (see Figure 25, green line). The obtained spectrum is comparable with the spectrum of pristine, doped PAn-e.[46] With exposure to HCl the band at 630 nm disappears, while the band at 310 nm shows a significant reduction in intensity. The disappearance of the former suggests the absence of the exciton in the polar lattice that is formed upon doping.[46] The decrease in the absorption of the latter suggests that the number of species undergoing the π-π* transition has decreased. Accompanying these changes two new bands are visible, one centered around 800 nm and the other at 400 nm. These peaks have been assigned to transition from the highest and the second highest valence bands to the polaron band situated in the middle of the bandgap.[46]

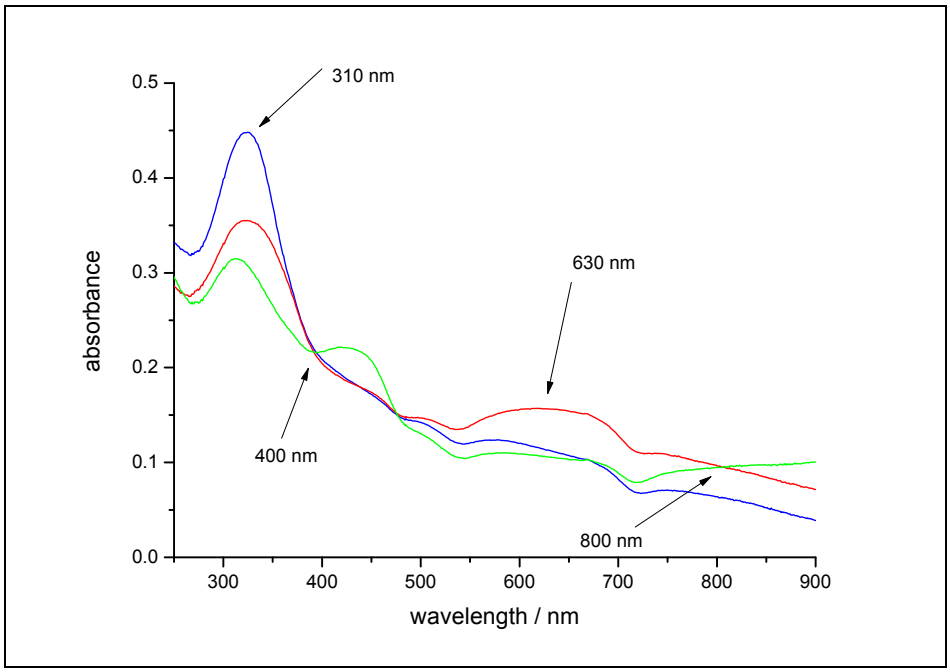

Figure 25: UV/Vis spectra of a thin film of FPAn-e before (blue line) and after irradiation (red line, mask aligner, 122.1 J/cm^2) and after treatment to gaseous hydrochloric acid (green line)

A kinetic study of the photo reaction was also carried out using the C=O vibration peak of the formamide group at 1670 cm^{-1}. For that reason thin films of FPAn-e were illuminated for defined periods, and absorbance FTIR spectra were recorded. An illumination for about 25 minutes leads to a conversion of about 80 % (see Figure 26). Further irradiation for 25 minutes causes only a slight decrease of the formamide groups.

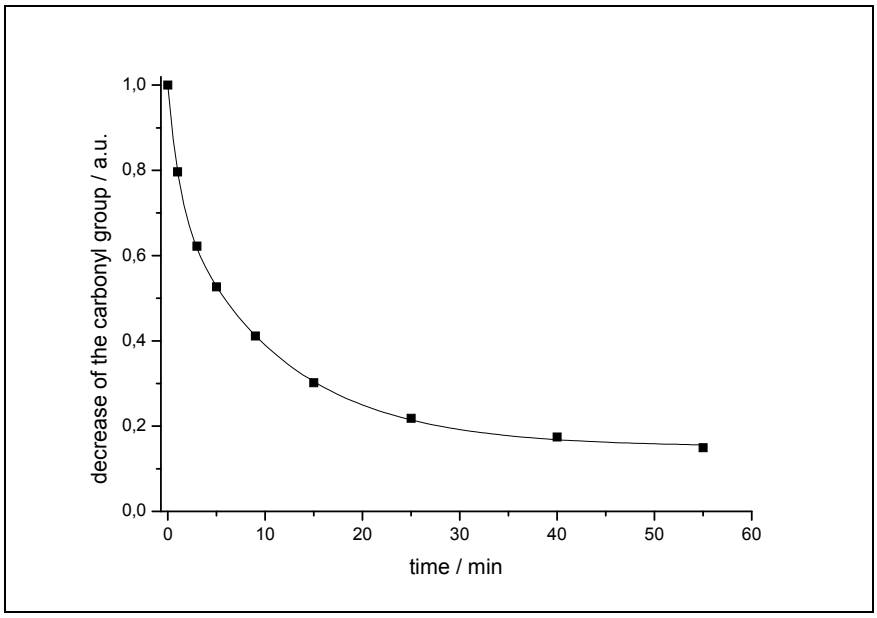

Figure 26: Kinetic study of the decarbonylation reaction of FPAn-e during irradiation with UV-light (λ= 270-353 nm, mask aligner, 122.1 J/cm^2). The fitted curve serves as guide to the eye.

4.3 Patterning of Thin Films of Poy-N-formyaniline Using Photolithographic Methods

In combination with lithographic methods, photosensitive FPAn-e can be applied for the generation of patterned polyaniline films. Therefore, thin films of FPAn-e were deposited on CaF_2 substrates by spincoating from FPAn-e - DMF solution. To create the pattern, thin films of FPAn-e were illuminated using a mask aligner system equipped with a suitable quartz-chromium mask (122.1 J/cm^2, λ=270-353 nm, contact lithography). The illuminated FPAn-e areas are clearly visible as dark blue features, see Figure 27. Without any optimisation, a resolution of 1 µm could be achieved in this experiment.

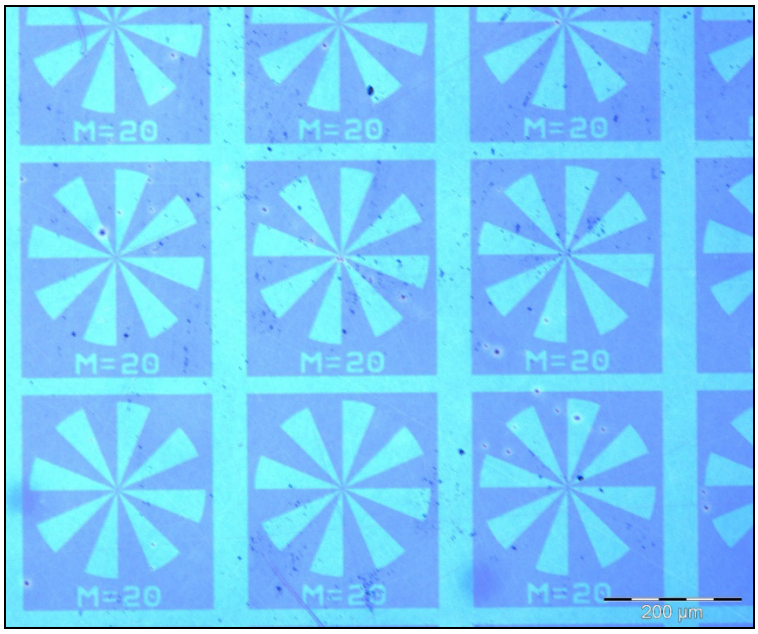

Figure 27: Patterned films of FPAn-e using a mask aligner (λ= 270-353 nm, 122.1 J/cm^2)

Moreover, the photogenerated polyaniline can be protonated as explained previously (chapter 4.2.2) leading to the green coloured and conductive polyaniline emeraldine salt. For that reason the photo patterned films were exposed to gaseous hydrochloric acid for about ten seconds which results in a change of the colour from dark blue to green in the illuminated areas as shown in Figure 28.

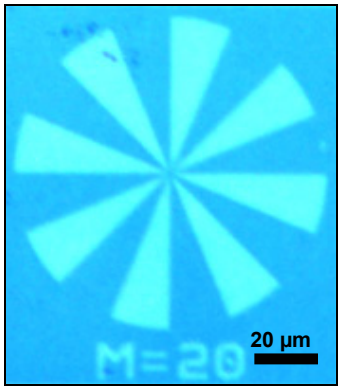

Figure 28: Patterned films of FPAn-e after exposure to gaseous hydrochloric acid.

4.4 Investigation of the Conductivity of Thin Films of Poly-N-formylaniline

4.4.1 CAFM-Measurements of Thin Patterned Films of Poly-N-formylaniline

Atomic force microscopy (AFM) allows a mapping of the surface topography with a lateral resolution in the range of few nanometres. AFM is one of the foremost tools for imaging, measuring, and manipulating matter at the nanoscale. Conductive atomic force microscopy (C-AFM) is a particular mode of AFM. This method provides the possibility of mapping the local film conductivity on the nanometre scale using conductive cantilevers. Conductive atomic force microscopy turned out to be an appropriate method to visualize the obtained contrast of the conductivity between the unilluminated and the illuminated/doped regions of the patterned samples.

For this experiment thin films of FPAn-e were deposited on conductive ITO and gold/glass substrates by spincoating from dimethyformamide solutions, respectively. In a next step these layers have been patterned using a mask aligner equipped with suitable chromium/quartz glass masks.

PAn-e on Au/glass substrate

After a subsequent exposure to gaseous hydrochloric acid, conductive atomic force microscopy (CAFM) was performed under ambient conditions. Figure 29a shows the obtained CAFM images in which the illuminated and doped regions offering high conductivity yield bright contrast, whereas the unilluminated areas with low conductivity exhibit darker contrast. This image reveals a significant difference in conductivity between both areas. However, in the topographical image (Figure 29b), no structural features resulting from the patterning and doping process are discernible.

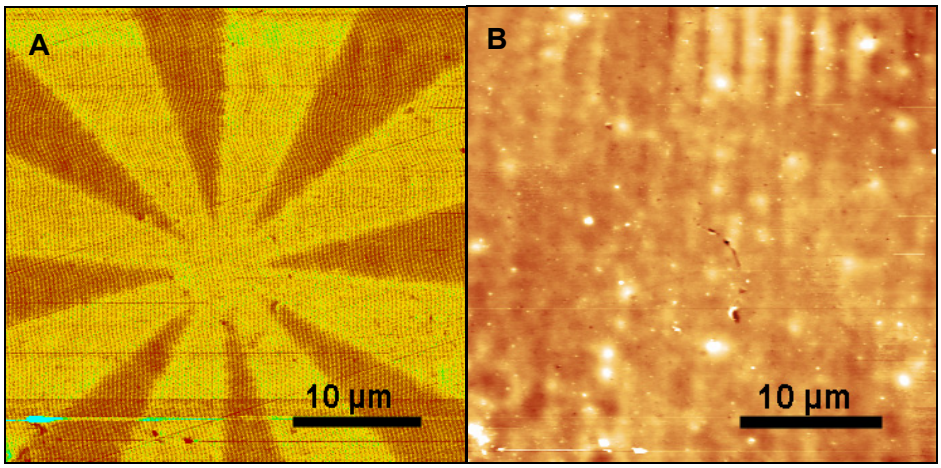

Figure 29: (a) C-AFM image and (b) height image of a patterned film of FPAn-e on a gold/glass substrate

PAn-e on ITO/glass substrate

In order to investigate both, the effect of the photoreaction and the effect of protonation on the conductivity, C-AFM measurements of the patterned polymer films on ITO/glass substrates were performed before and after protonation. Moreover, to evaluate the stability of the protonated areas under UV-iumination further C-AFM measurements were conducted after an additional irradiation for 55 minutes (122.1 J/cm^2).

Figure 30 shows the obtained C-AFM images in which the illuminated regions offering high conductivity yield bright contrast, whereas the unilluminated areas with low conductivity exhibit darker contrast. Interestingly, the conductivity also increases in the illuminated region direct after UV irradiation. This effect can be attributed to the electron withdrawing effect of the formyl groups in the unexposed areas. In general, N-acyl polyanilines are less conducting than the pristine, undoped PAn-e due to the depletion of electron density on the polymeric chains. Moreover, a significant change in the height image can be observed which is in sharp contrast to the measurements which were performed on gold/glass substrates.

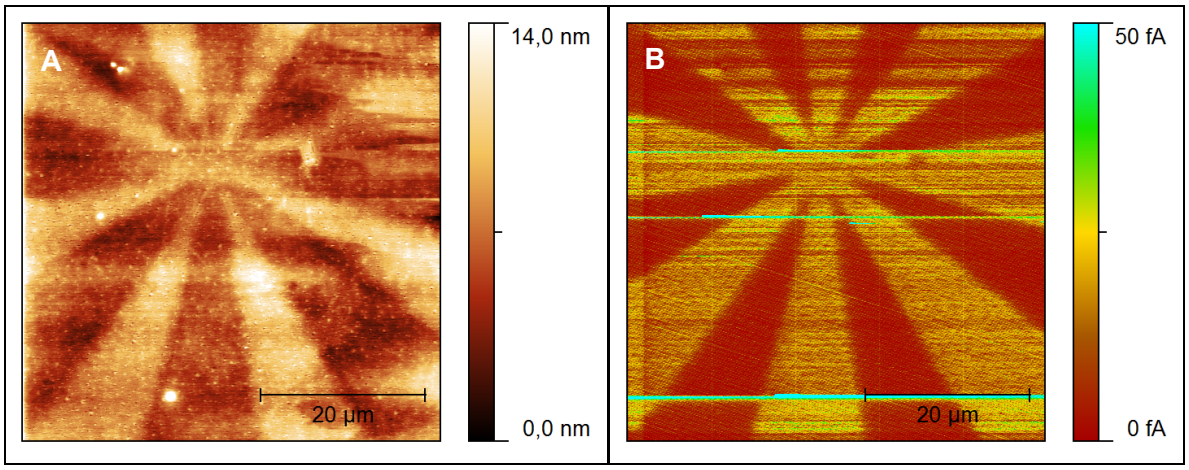

Figure 30: (a) Height image and (b) C-AFM image of a patterned film of FPAn-e on an ITO/glass substrate

A protonation with gaseous hydrochoric acid result in a drastic increase of the conductivity of the irradiated areas which is depicted in Figure 31a. Figure 31a, shows the measured C-AFM image in which the illuminated and protonated regions offering high conductivity yield dark contrast, whereas the unilluminated areas with low conductivity exhibit brighter contrast.In comparison with Figure 30b, the C-AFM result in Figure 31a, exhibit a sharper contrast which can be attributed to more pronounced difference in conductivity between both areas.

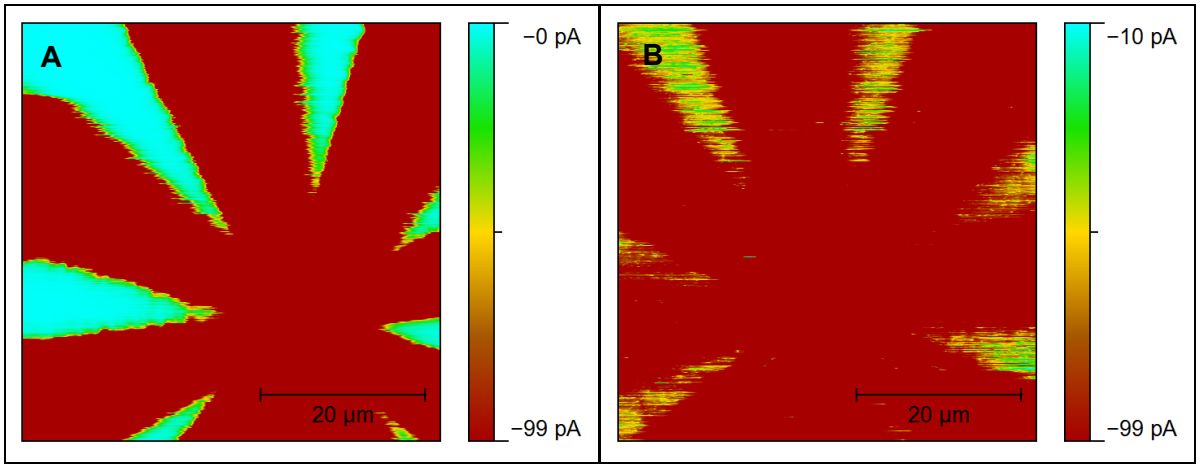

Figure 31: C-AFM images of a patterned film of (a) FPAn-e on an ITO substrate upon exposure to gaseous hydrochloric acid and (b) a subsequent post illumination with UV light for 122.1 J/cm^2.

A subsequent illumination with UV light for 55 min (122.1 J/cm^2) (as shown in Figure 31, b) leads to a slight increase in conductivity of unprotonated areas which can be attributed to the

loss of the formyl groups as explained previously. However, the conductivity of the protonated areas is not influenced by the post illumination.

Summing up, the photoreaction and a subsequent protonation lead to a significant change in the conductivity in the UV illuminated areas. Moreover, the protonated and conductive areas are stable under UV illumination.

This fact offers the possibility for the fabrication of conductive pattern of polyaniline embedded in a non-conductive matrix of polyaniline as required for electrodes and interconnects in various organic electronic devices.

4.4.2 Investigation of the Dependence of the Sheet Conductivity on the Conversion of the Photoreaction

The photoreaction of FPAn-e provides a versatile and convenient method for achieving a modulation of the conductivity. The changes in sheet conductivity of these FPAn-e films were measured using a two point measurement setup. Therefore a thin film of FPAn-e on a CaF_2 substrate was patterned illuminated using different irradiation periods and was subsequently exposed to gaseous HCl.

For comparison the conductivity of a thin layer of acid doped, pristine PAn-e was also investigated. Due to the fact that the absolute conductivity depends on several parameters i.e. the dopant and the molecular weight the measured conductivities have been referred to the value of the doped, pristine PAn-e. Figure 32 shows the dependence of the relative sheet conductivity of thin films of FPAn-e with the illumination time.

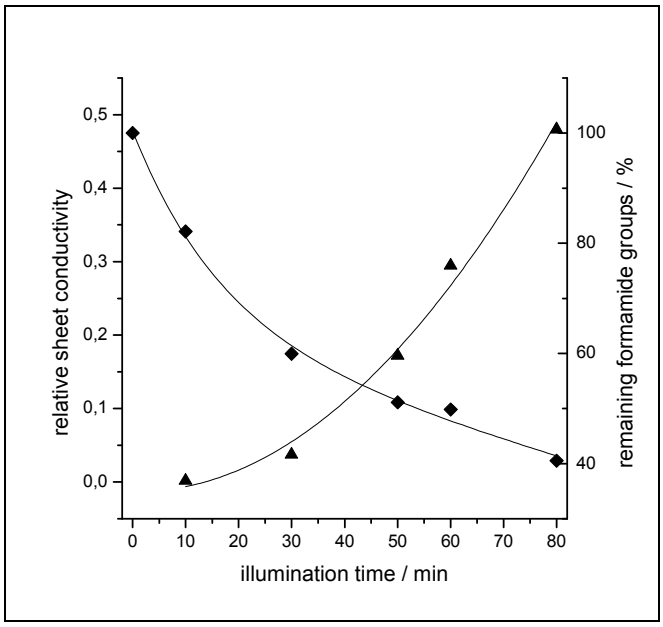

Figure 32: Comparison of the relative sheet conductivity (points) with the decrease of the carbonyl groups (rectangles) dependent on the irradiation time (irradiation with medium pressure mercury lamp, λ= 260-320 nm, E = 180 mW/cm^2). The fitted curves serve as guide to the eye.

In Figure 32 also the conversion of the formamide units during UV illumination (260-320 nm; 180 mW cm^{-2}), which was calculated from the depletion of the carbonyl vibration signal at 1673 cm^{-1}, is depicted. After exposure with an energy density of 864 J cm^{-2}, 60 % of all N-formyl units have been converted leading to a sheet conductivity of about 50 % of pristine, doped PAn-e. This result is in contrast to the results obtained with PAn/PAG blends in which conductivities of about one magnitude lower than in pristine, doped PAn have been reported. Moreover, the ionic moieties of the decomposed PAG in such blend might also raise problems in organic devices i.e. influences the stability of the obtained PAn pattern under operating conditions.

4.5 Application of Poly-N-formylaniline as Negative-toned Resist

Due to the fact that the generated emeraldine salt which is formed after protonation with gaseous hydrochloric acid in the illuminated areas of thin films of FPAn-e is largely insoluble in organic solvents, patterned films of doped polyaniline can be obtained upon a subsequent development step. Thus the FPAn-e can be applied as negative- tone photoresist.

To create such a pattern, a thin film of FPAn-e was illuminated using a mask aligner system and a suitable quartz-chromium mask (contact lithography, 122.1 J/cm^2). The illuminated FPAn-e areas are clearly visible as dark blue features, see Figure 33a. Without any optimisation, a resolution of 1 µm was achieved in this experiment. An exposure to gaseous hydrochloric acid leads to the formation of the green polyaniline emeraldine salt as shown in Figure 33b. A subsequent development with dimethylformamide causes the dissolving of the unexposed areas as shown in Figure 33c.

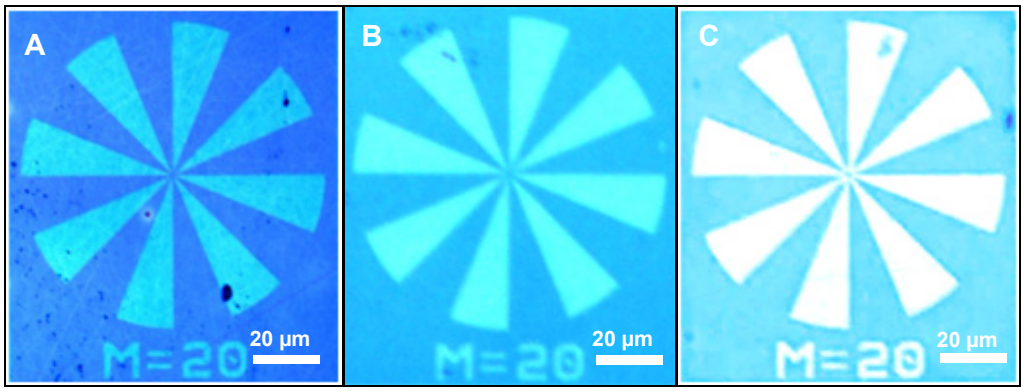

Figure 33: Thin films of FPAn-e upon (a) patterned illumination with UV-light (mask aligner, 122.1 J/cm^2) and (b) after subsequent treatment with gaseous hydrochloric acid, and (c) after subsequent development with dimethylformamide.

4.6 Application of Thin Poly-N-formylaniline Films as Hole Transport Layer in Organic Light Emitting Diodes (OLEDs)

In an additional experiment photogenerated PAn-e as hole transport layer in organic light emitting devices (OLED) was tested. In general pristine PAn-e can be applied as hole transport layer in OLEDs as reported in literature.[47] For that reason a simple OLED was assembled on an indium-tin oxide (ITO) coated glass substrate. The build-up is schematically depicted in Figure 34.

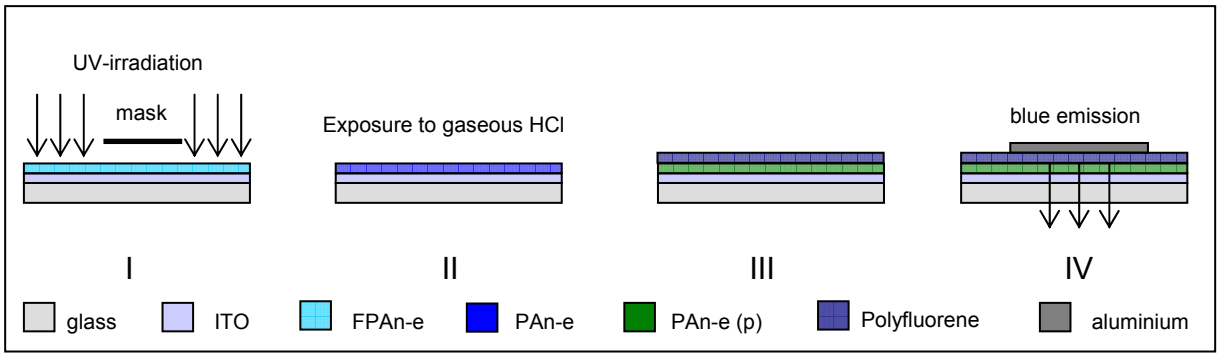

Figure 34: Scheme of the preparation of an OLED using FPAn-e as hole transport layer

The transparent ITO electrode was covered with a thin film of FPAn by spin casting from DMF solutions. In a further step the FPAn-e layer was illuminated with UV-light (270-353 nm, mask aligner, 122.1 J/cm^2) and protonated with gaseous hydrochloric acid. Subsequently a thin layer of polyfluorene was deposited also by spin casting from a dichloromethane solution as an emissive material. Finally, on top of this device a layer of aluminum was evaporated (contact electrode). Figure 35 shows the blue electroluminescence of this device when operated at 18 V.

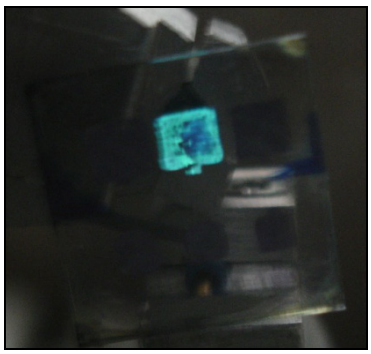

Figure 35: Photograph of the OLED

A more detailed investigation of FPAn-e as hole transport layer and the fabrication of patterned devices are subjects of current research.

5 Conclusions

In this thesis two photosensitive polyaniline derivatives bearing N-formamide groups have been synthesized. Using the conductive polymers PAn and POT as starting materials, two photosensitive N-formyl derivatives could be obtained by a polymer analogous formylation reaction using a mixture of acetanhydride and formic acid as formylation agent. POT was chosen due to its better solubility in organic solvents.

Upon irradiation with UV light the N-formamide groups in the investigated polymers undergo a photodecarbonylation reaction. Figure 36 displays these photoreactions in the different polymers. Because of this significant change in the chemical structure of the polymers, the photoreaction can be easily followed by spectroscopic methods such as UV/VIS and FTIR spectroscopy.

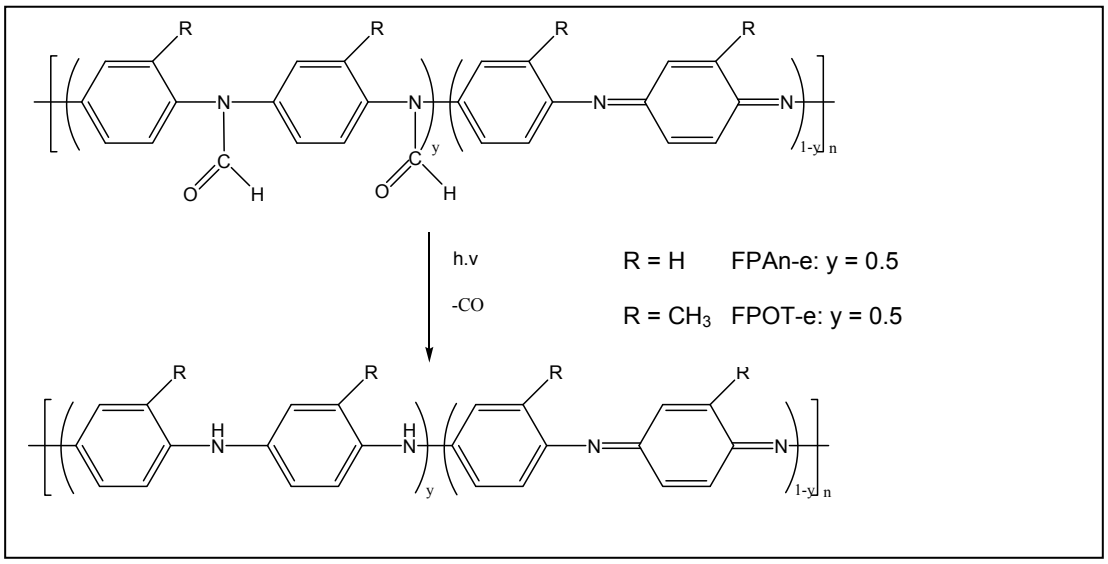

Figure 36: Decarbonylation reaction in the investigated polymers.

The measured spectroscopic data reveal that the photodecorbonylation reaction of FPAn-e results in the formation of PAn-e. In case of FPOT-e it turned out that the photoreaction does not lead to the expected POT in its emeraldine form.

For that purpose a photolithographic patterning of thin films of FPAn-e using a mask aligner equipped with suitable quartz/chromium masks was performed. The illuminated FPAn-e areas are clearly visible as dark blue features, see Figure 37 a. Without any optimisation, a

resolution of 1 µm could be achieved in this experiment. It turned out that the photogenerated PAn-e provides the properties of pristine PAn-e. Thus it can be protonated with gaseous hydrochloric acid which results in the dark green pattern shown in Figure 37.

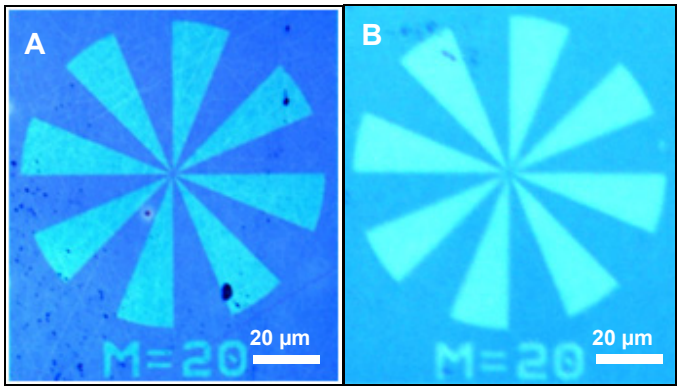

Figure 37: Thin films of FPAn-e on CaF_2 substrates after (a) patterned illumination with UV-light and (b) after a subsequent treatment with gaseous hydrochloric acid.

In addition, the protonation of the illuminated areas leads to a significant increase in conductivity as known for pristine PAn-e. In contrast, the unilluminated areas remain non-conductive, which offers the possibility of patterned, conductive polyaniline films.

In order to visualize the obtained contrast of the conductivity, conductive atomic force microscopy (C-AFM) was performed on the patterned films. Figure 38 shows the obtained C-AFM images in which the illuminated and doped regions offering high conductivity yield bright contrast, whereas the unilluminated areas with low conductivity exhibit darker contrast. This image reveals a significant difference in conductivity between both areas. However, in the topographical image (Figure 38), no structural features resulting from the patterning and doping process are discernible.

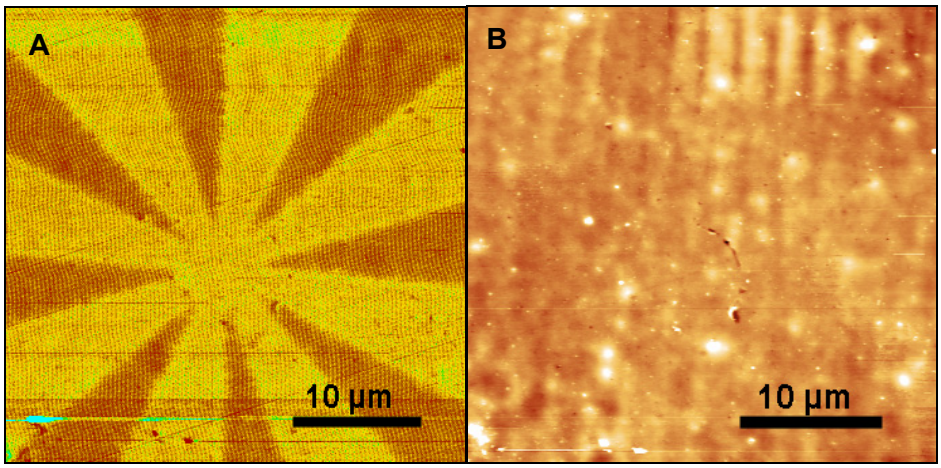

Figure 38: (a) C-AFM image and (b) height image of a patterned film of FPAn-e on a gold/glass

The changes in sheet conductivity of these FPAn-e films were measured using a two point measurement setup. Therefore a thin film of FPAn-e on a CaF_2 substrate (see Figure 39) was patterned illuminated using different irradiation periods and was subsequently exposed to gaseous HCl.

It turned out that the relative sheet conductivity of thin films of FPAn-e depends on the degree of the photoconversion.

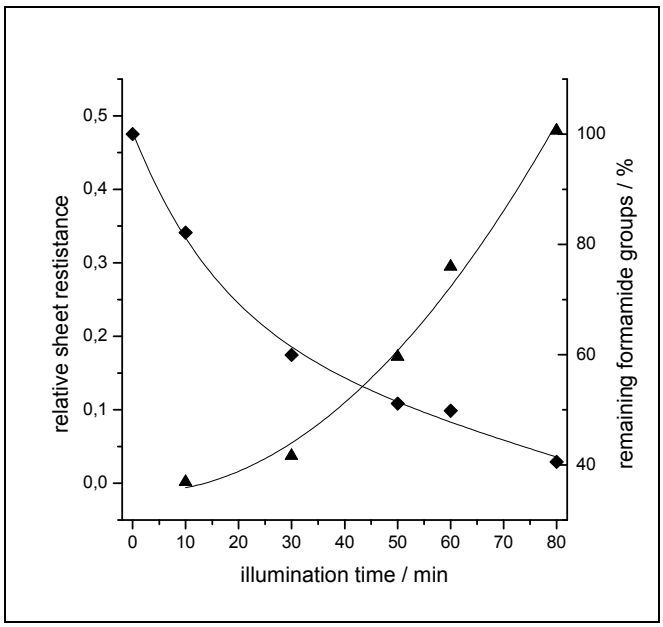

Figure 39: Comparison of the relative sheet conductivity (points) with the decrease of the carbonyl groups (rectangles) dependent on the irradiation time. The fitted curves serve as guide to the eye.

Figure 39 shows the dependence of the relative sheet conductivity and the conversion of the photoreaction with the illumination time.

Due to the fact that the generated emeraldine salt which is formed after protonation with gaseous hydrochloric acid in the illuminated areas of thin films of FPAn-e is largely insoluble in organic solvents, patterned films of doped polyaniline can be obtained upon subsequent development with dimethylformamide as shown in Figure 40. Thus the FPAn-e can be applied as negative-toned photoresist.

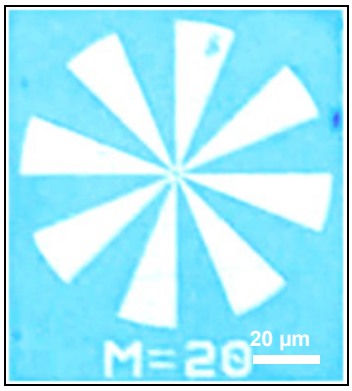

Figure 40: Patterned films of FPAn-e after a treatment with gaseous hydrochloric acid and after a subsequent development with dimethylformamide.

In a further approach thin films of photogenerated PAn-e were applied as hole conductive layer in organic light emitting diodes. For that reason a simple OLED was assembled on an indium-tin oxide (ITO) coated glass substrate. Figure 41 shows the blue electroluminescence of this device when operated at 18 V.

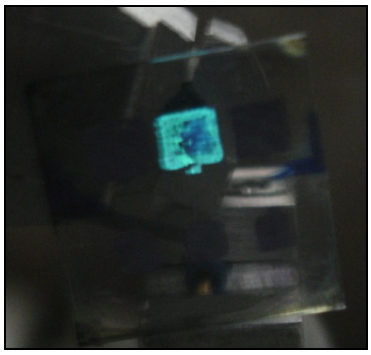

Figure 41: Photograph of the OLED

6 Experimental

6.1 Chemicals

All chemicals (see Table 1) were used without proving the purity, which was indicated by the producer, and without further purification.

Table 1: List of used chemicals

Chemical	Producer	Purity
Acetic anhydride	Sigma	p.a.
Ammonium hydroxide	Fluka	puriss p.a.
Ammonium sulfate	Sigma Aldrich	purum p.a.
1,4 Dioxane	Sigma Aldrich	absolute
Ferrous(II) sulfate	Merck	p.a.
Formic acid	Merck	p.a.
Hydrochloric acid (32 %)	Fluka	puriss p.a.
Methanol	Fluka	puriss.: absolute; over molecular sieve (H_2O < 0.01 %)
Methylene chloride	Sigma	absolute; over molecular sieve (H_2O < 0.01 %)
N,N-Diethylhydroxylamine	Aldrich	≥ 98 %
N,N-Dimethylformamide	Roth	≥ 99.5 %
N,N-Dimethylformamide (anhydrous)	Sigma Aldrich	99 %
o-Toluidine	Sigma	99.00 %
Polyaniline	Aldrich	
Tetrahydrofuran, anhydrous	Sigma	99.9 %
Trichloromethane	Roth	puriss p.a.

6.2 Instruments and Methods

6.2.1 Gel Permeation Chromatography

The weight and number average molecular weights (MW and Mn) as well as the polydispersity index (PDI) were determined by gel permeation chromatography with N-methyl-2-pyrrolidone (NMP) as solvent using the following arrangement: Merck Hitachi L6000 pump, separation columns of Polymer Standards Service, 8 x 300 mm STV 5 µm grade size (106 Å, 104 Å, and 103 Å), combined refractive index – viscosity detector from Viscotec, Viscotec 200. Polystyrene standards purchased from Polymer Standard Service were used for calibration.

6.2.2 Infrared Spectroscopy

FT-IR spectra were recorded with a Perkin Elmer “Spectrum One” instrument (spectral range between 4000 and 450 cm^{-1}). All FTIR spectra were recorded in transmission mode.

6.2.3 UV/Vis Spectroscopy

UV/VIS spectra were measured with a Varian Cary 50 UV/VIS spectrophotometer. All UV/VIS spectra were taken in the absorbance mode.

6.2.4 ^{1}H-NMR-Spectroscopy

^{1}H-NMR and ^{13}C-NMR spectra were recorded with a Varian 400-NMR spectrometer operating at 399.66 MHz and 100.5 MHz, respectively, and were referenced to Si(CH3)4. A relaxation delay of 10 s and 45 pulse were used for acquisition of the ^{1}H-NMR spectra.

Solvent residual peaks were used for referencing the NMR spectra to the corresponding values given in literature.[48]

6.2.5 Conductive Atomic Force Microscopy

C-AFM measurements were carried out using a Digital Instruments (DI) Multi mode 3, with a self-build C-AFM amplifier. The measurements were performed by Andreas Pavitschitz, Institute of Physics (University of Leoben). All measurements were conducted in contact mode. The used cantilever was a TiN coated single crystal n-doped Si cantilever from NT-MDT, which is a very long and soft cantilever.

6.3 Synthesis of the Polymers

6.3.1 Poly-*o*-toluidine (emeraldine base)

POT-e was synthesised according to a literature protocol.[35]

Poly-o-toluidine (emeraldine salt)

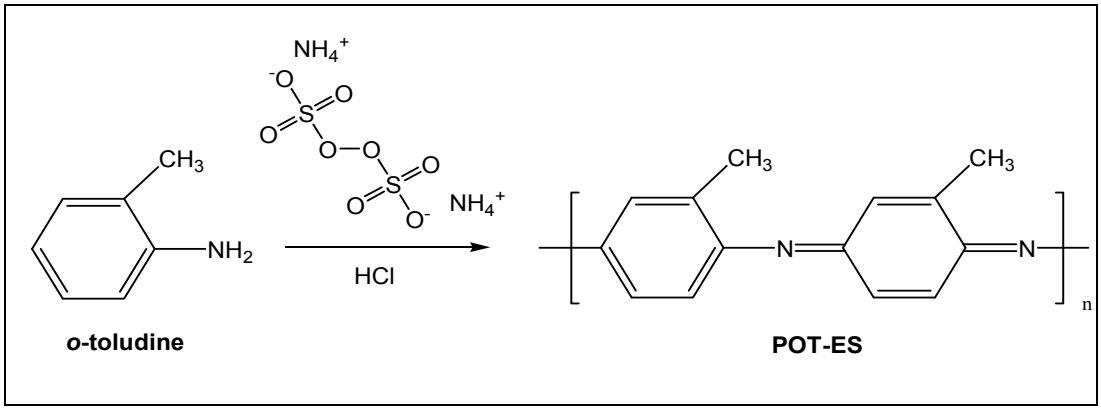

O-toluidine (10.7 g; 100 mmol) was dissolved in 300 mL of 1 M hydrochloride acid under ice cooling. In addition a catalytic amount of ferrous sulfate was added to the solution. In a next step a cooled solution of ammonium sulfate (4.6 g; 34.8 mmol) in 100 mL of 1 M hydrochloride acid was added dropwise to the solution of *o*-toluidine over ten minutes under stirring. A change of the colour of the solution from light orange to dark green could be

observed. After adding of all of the solution of ammonium sulfate the mixture was cooled for two hours in the refrigerator. The precipitated polymer was filtered off and subsequently washed with about 300 mL of 0.1 M HCl. Afterwards the polymer was dried for 48 hours in the vacuum oven.

Yield: 3.688 g of a very deep green solid

Poly-o-toluidine (emeraldine base) (POT-e)

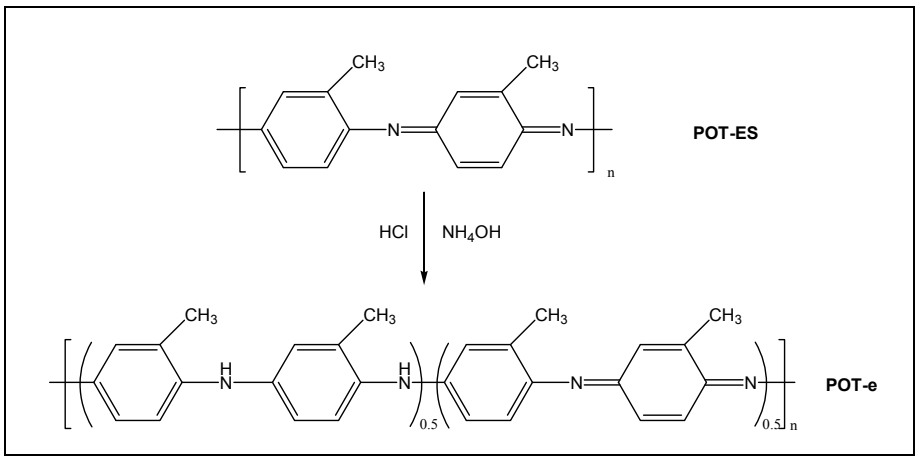

In order to convert the salt form into the insulating base form, the dried salt form (3.688 g) was stirred for 48 hours in 400 mL of an aqueous solution of 0.1 M ammonium hydroxide. The obtained insulating base form was filtered off, washed with a mixture of methanol and 0.2 M NH_4OH (1:1) and dried in the vacuum oven for 48 hours.

Yield: 910.3 mg of a deep blue to black coloured solid

^{1}H-NMR (400 MHz, 20°C, $CDCl_3$) δ 6.4-7.5 (m, 3H, Ph); 4.8-5.7 (s, 1H, NH); 1.9-2.4 (m, 3H, CH_3).

FT-IR (CaF_2, cm^{-1}): 3384, 1600, 1490, 1306, 1248, 1109, 1001, 886.

6.3.2 Poly-N-fomyl-o-toluidin (emeraldine base)

Poly-N-fomyl-o-toluidine (emeraldine base) (FPOT-e)

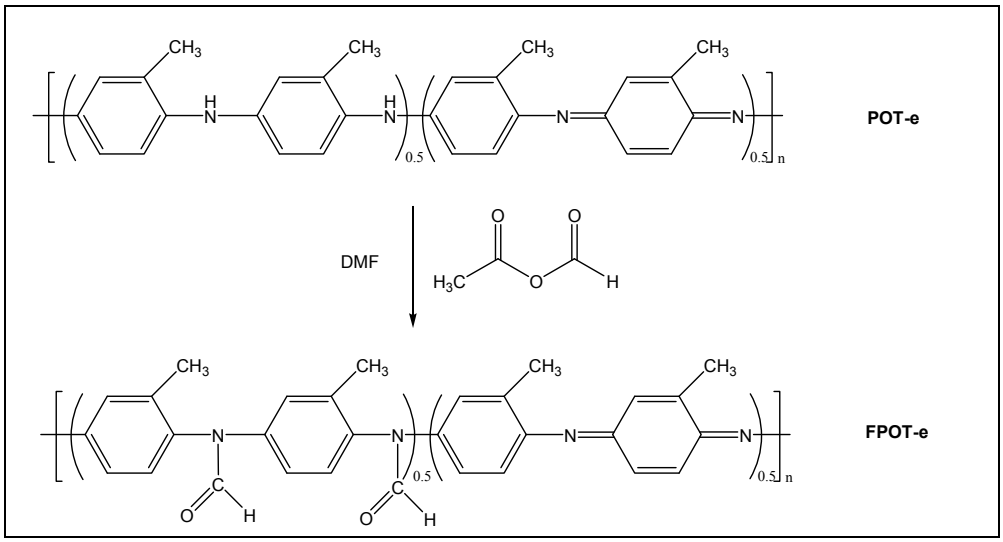

In a first step 4 mL of acetic anhydride and 2 mL of formic acid were mixed.

To a solution of 200 mg of POT-e in 20 mL THF (anhydrous) the mixture of acetanhydride and formic acid was added under stirring. The reaction was stirred at 50°C for 48 hours under exclusion of light. The colour of the mixture turned slowly from dark blue into reddish brown. Then the product was precipitated by adding 20 ml ammonium hydroxide solution (10 %). After for hours stirring the precipitate was filtered rinsed with distilled water. The product was dried in the vacuum oven at 50°C.

Yield: 189.6 mg of a brown solid

6.3.3 Poly-*o*-toluidine (leucoemeraldine base)

Poly-o-toluidine (leucoemeraldine base) (POT-l)

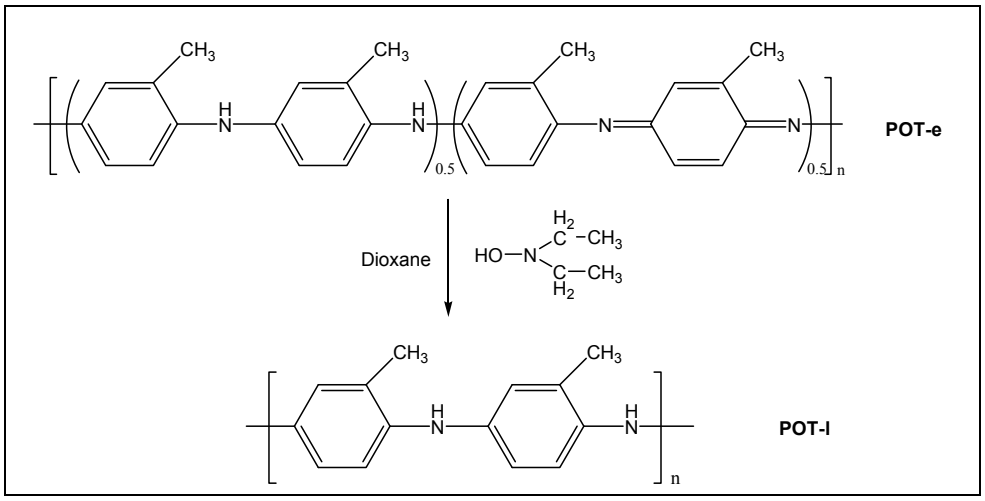

The reduction was performed in nitrogen atmosphere using the schlenk technique. 100 mg of POT-e were dissolved in 30 mL of dioxane. 15 mL of *N,N*-diethylhydroxylamine (reducing agent) were added to the solution. The reaction was stirred at 80°C for several hours. The colour of the solution changed to a clear, light yellow liquid.

The solvent was removed by vacuum distillation. The polymer was precipitated by dropping the solution into a tenfold excess of degassed distilled water. Afterwards the product was dried in the vacuum oven 70°C for two hours. The obtained polymer was dissolved in 5 ml dichloromethae and subsequently precipitated by dropping the solution into a tenfold excess of absolute methanol. The colour of the suspension turned into light blue. In a next step the polymer was filtered off and dried in the vacuum oven at 70 over night.

Yield: 85 mg of a brown solid

6.3.4 Poly-N-fomyl-o-toluidin (leucoemeraldine base)

Poly-N-fomyl-o-toluidin (leucoemeraldine base) (FPOT-l)

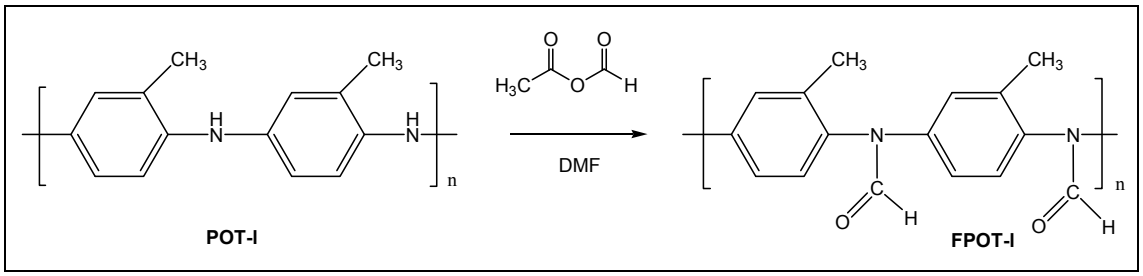

In a first step 1 mL of acetic anhydride and 0.5 mL of formic acid were mixed.

To a solution of 10 mg of POT-e in 10 mL dioxane (anhydrous) the mixture of acetanhydride and formic acid was added under stirring. The reaction was stirred at 50°C for 48 hours under exclusion of light. Then the product was precipitated by adding 5 ml ammonium hydroxide solution (10 %). After four hours stirring the precipitate was filtered and rinsed with distilled water. The product was dried in the vacuum oven at 50°C.

Yield: 5 mg of a brown solid

6.3.5 Poly-N-formylaniline (emeraldine base)

Poly-N-formylaniline (emeraldine base) (FPAn-e)

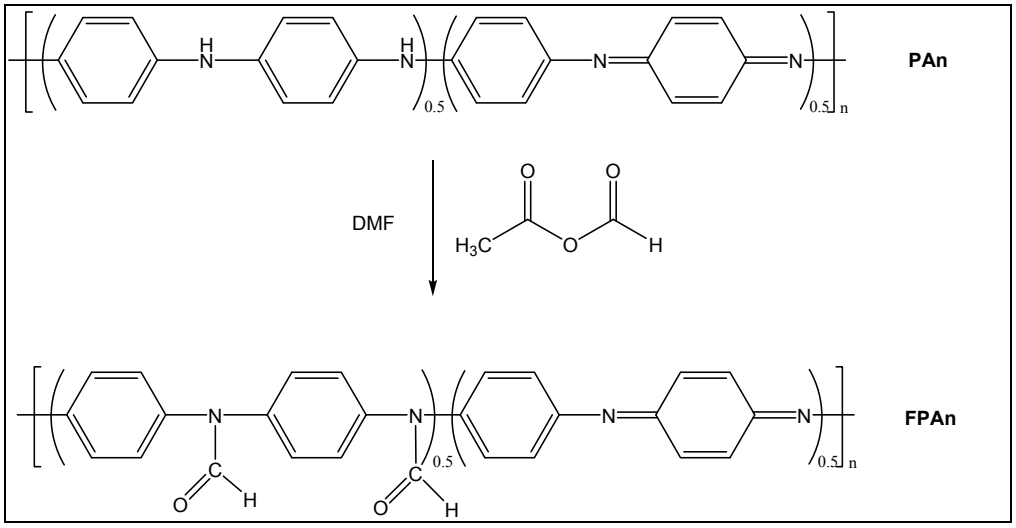

In a first step 2 mL of acetic anhydride and 1 mL of formic acid were mixed.

To a solution of 100 mg of POT-e in 50 mL dimethylformamide (anhydrous) the mixture of acetanhydride and formic acid was added under stirring. The reaction was stirred at 50°C for 48 hours under exclusion of light. The colour of the mixture turned slowly from dark blue into dark brown to black. Then the product was precipitated by adding 20 ml ammonium hydroxide solution (10 %). After four hours stirring the precipitate was filtered and rinsed with distilled water. The product was dried in the vacuum oven at 50°C.

Yield: 69.6 mg of a dark brown solid.

6.4 Preparation of Thin Poly-N-formylaniline Films on CaF_2-, Au/Glass- and ITO/Glass- Substrates

Thin films of the investigated polymers were coated on various substrates using the Photo Resist Spinner (Model 4000, Electronic Micro Systems).

For irradiation experiments and spectroscopic measurements CaF_2 substrates were used due to their high optical transparency in the infrared and UV/VIS range, respectively.

For CAFM measurements and for the assembly of the OLED ITO substrates (CG-61IN) with dimensions of 15 x 15 mm produced by Delta Technologies were used. The ITO layer was deposited by a sputtering process on glass. ITO substrates are highly conductive (15-30 Ω) and transparent in the visible range.

Additional CAFM measurements were carried out on gold/glass substrates. For the preparation of these substrates chromium was deposited as an adhesive layer by thermal evaporation on precleaned glass substrates using a Balzers MED010. In a next step a gold layer was deposited also by thermal evaporation.

Thin films of POT-e, POT-l, FPOT-e and FPOT-l were prepared by spin casting from THF solutions. Due to the poor film forming properties of FPAn-e, the ITO/glass, CaF_2 and gold/glass substrates were preheated to 120°C for 30 minutes. The deposition of the FPAn-e layer was performed by spincoating from dimethylformamide solutions (30 mg FPAn-e in 1 ml of dimethylformamide). In addition the FPAn-e/DMF solution was heated to 50°C before deposition. In Table 2 the used spin coat parameter for the different substrates were listed.

Table 2: Schedule of the settings for spin casting

Polymer specific			Spin cast dates		
polymer	**solvent**	**substrate**	**speed / rpm**	**ramp / rpm s^{-1}**	**dwell / s**
FPOT (10 mg/mL solvent)	Methylene chloride	CaF_2 Ø 20 mm	500	100	50
FPAn-e (10-30 mg/mL solvent)	DMF	CaF_2 Ø 20 and 30 mm	250 250	5 5	800 800
FPAn-e (10 mg/mL solvent)	DMF	gold/glass (10 x 10 mm)	500	10	800
FPAn-e (10 mg/mL solvent)	DMF	ITO/glass (10 x 10 mm)	500	10	800
PF (10 mg/mL solvent)	Trichloromethane	ITO/glass (10 x 10 mm)	300	10	20

6.5 Irradiation of the Investigated Photoreactive Polymers

UV-irradiation experiments were carried out with a medium pressure Hg lamp (100 W, from Newport, model 66990) equipped with a filter for the range of 260 - 320 nm. In these experiments, the light intensity (power density) at the sample surface was measured with a spectroradiometer (Solatell, Sola Scope 2000TM, spectral range from 230 to 470 nm) to be 180 mW cm^{-2} in the range of 260-320 nm. All UV illuminations were carried out under inert gas atmosphere (N_2). Caution: UV irradiation causes severe eye and skin burns. Precautions (UV protective goggles, gloves) must be taken! Photolithographic patterning was carried out with a mask aligner (model MJB4 from SUSS, Germany) using a 500 W HgXe lamp equipped with a filter transmissive for the wavelength range from 270 nm to 353 nm and a light intensity of 37 mW cm^{-2}.

6.6 Doping of the Irradiated Polymer Films with Gaseous Hydrochloric Acid

The protonation of the photogenerated PAn-e was performed by gaseous hydrochloric acid. For that purpose the polymer layer was exposed to vapours of a conc. HCl solution for 20 seconds at room temperature.

6.7 Developing of Patterned Poly-N-formylaniline Films Using Dimethylformamide

Patterned FPAn-e films on CaF_2 substrates were protonated as described in the previous section and were subsequently immersed in dimethylformamide for five seconds.

6.8 Determination of the Sheet Conductivity

Conductivity measurements were performed with of a Keithley 2400 instrument using a two point measurement setup. In order to perform the conductivity measurements of the illuminated FPAn-e at a constant film thickness, one sample was patterned illuminated using different irradiation periods. Upon exposure to gaseous hydrochloric acid thin Al-electrodes were deposited via evaporation with a Balzers MED010 on the illuminated and doped areas (see Figure 42. The channel width between both Al-electrodes was 0.1 mm. The resistance of the different illuminated polymer areas was measured. Table 3 shows the calculated relative sheet conductivities of the different illuminated areas.

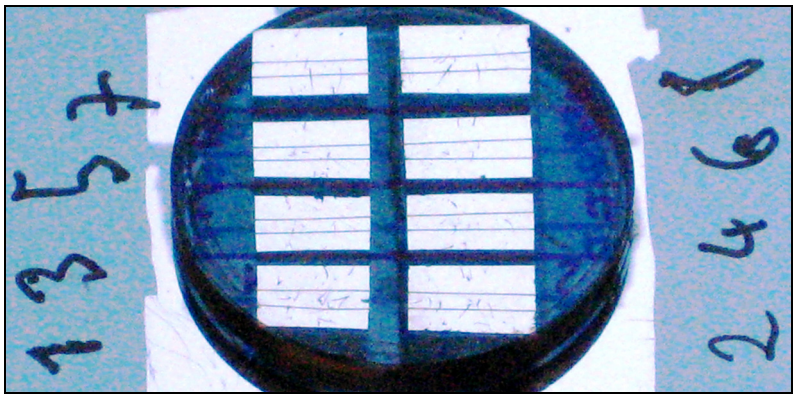

Figure 42: Photograph of the preparation of the sample for conductivity measurements

Table 3: Determination of the relative sheet conductivity.

Area	Illumination period / min	resistance / MΩ	length / mm	**Rel. sheet conductivity**
1	10	960	6,96	0,00192
3	30	45,9	7,14	0,03755
5	50	10	7,15	0,17214
6	60	5,4	7,73	0,29485
8	80	3,3	7,77	0,48
pristine doped PAn		1,6	7,69	1

6.9 Assembly of Organic Light Emitting Diodes

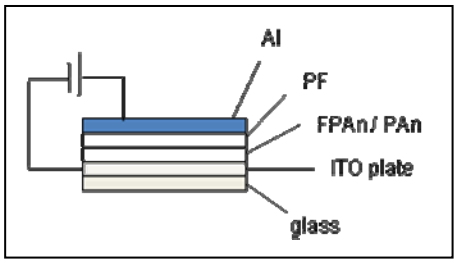

Figure 43: Assembly of the OLED

The transparent ITO electrode was covered with a thin film of FPAn-e by spin casting from DMF solutions (10 mg/ml see section 6.4). In a further step the FPAn-e layer was illuminated with UV-light (λ= 270-353 nm, mask aligner, 122.1 J/cm^2) and protonated with gaseous hydrochloric acid (see section 6.6). Subsequently a thin layer of polyfluorene (10 mg/ml) was deposited also by spin casting from dichloromethane solution. Finally, on top of this device a layer of aluminum was deposited by thermal evaporation using a Balzers MED010 (contact electrode).

7 Appendix

7.1 List of Figures

7.2 List of Abbreviations

AFM	Atomic force microscopy
Al	Aluminium
Au	gold
°C	degree Celsius
CaF_2	Calcium fluoride
C-AFM	Conductive atomic force microscopy
cm	centimeter
cm^2	square centimeter
DMF	*N,N*-Dimethylformamide
e.g.	exempli gratia, for example
et al.	et alii/aliae/alia (lt.), and others
etc.	et cetera (lt.), and so on
fA	femtoampere
FPAn-e	Formylated Polyaniline (emeraldine base)
FPOT	Formylated Poly-*o*-toluidine

FTIR	Fourier transform infrared spectroscopy
H_2O	Water
HCl	Hydrochloride acid
IR	infrared
ITO	Indium tin oxide
mg	milligram
min	minutes
mL	milliliter
mm	millimeter
mW	milliwatt
nm	nanometer
NMR	Nuclear magnetic resonance
p.a.	pro analysi (lt.), for synthesis
pA	picoampere
PAG	Photo acid generator
PAn-e	Polyaniline (emeraldine base)
PF	Polyluorene
POT	Poly-*o*-toluidine
POT-e	Poly-*o*-toluidine (emeraldine base)
POT-l	Poly-*o*-toluidine (leucoemeraldine base)
Si	Silicium
TiN	Titanium nitride
UV	Ultraviolet
UV/Vis	Ultraviolet-visible
µm	micrometer

7.3 List of Tables

Table 2: Schedule of the settings for spin casting

7.4 References

[1] H.S. Nalwa, Ed., „*Handbook of Organic Conductive Molecules and Polymers*“, John Wiley & Sons Inc., Chichester 1997, Vol. I-IV.

[2]J.A. Chilton and M.T. Goosey, *“Special Polymers for Electronics and Optoelectronics”*, Chapman & Hall, 1995, p. 1-2.

[3] A. G. Green, A. E. Woodhead, *J. Chem. Soc.* **1910**, 1117.

[4] A. Ray, G. E. Asturias, D. L. Kershner, A. F. Richter, A. G. MacDiarmid, A. J. Epstein, *Synth. Met.* **1989**, *29*, E141.

[5] E. T. Kang, K. G. Neoh, K. L. Tan, *Surf. Interface Anal.* **1992**, *19*, 33.

[6] H. J Letheby, *Chem. Soc.* **1862**, *15*, 161.

[7] G.H. Gelinck, T.C.T. Geuns, D.M. de Leeuw, *Appl. Phys. Lett*. **2000**, *77*, 1487.

[8] Y.-C. Li, Y.-J. Lin, H.-J. Yeh, T.-C. Wen, L.-M. Huang, Y.-K. Chen, Y.-H. Wang, *Appl. Phys. Lett.* **2008**, *92***,** 093508.

[9] G. Gustafsson, Y. Cao, G.M. Treacy, F. Klavetter, N. Colaneri, A. J. Heeger, *Nature* **1992**, *357*, 477.

[10] H. Karamia, M. F. Mousavia, M. Shamsipurb, *J. Power Sources* **2003**, *117*, 255.

[11] K. S. Ryua, K. M. Kima, S.-G. Kanga, G. J. Leeb, J. Jooc, S. H. Changa, *Synthetic Metals* **2000**, *110*, 213.

[12] L. Zhao, L. Zhao, Y. Xu, T. Qiu, L. Zhi, G. Shi, *Electrochimica Acta* **2009**, *55*, 491.

[13] D. DeLongchamp, P. T. Hammond, *Adv. Mater*. **2001**, *13*, 1455.

[14] C. Marcel, J.-M. Tarascon, *Solid State Ionics* **2001**, *143*, 89.

[15] J. Huang, S.Virji, B. H. Weiller, R. B. Kaner, *J. Am. Chem. Soc.*, **2003**, *125*, 314.

[16] S. Virji, J. Huang, R. B. Kaner, B. H. Weiller, *Nano Letters* **2004**, *4*, 491.

[17] M. Leclerc, J. Guay, L. H. Dao, *Macromolecules* **1989**, *22*, 649.

[18] W. Barford, *“Electronic and Optical Properties of Conjugated Polymers”*, Oxford University Press Inc., New York, 2005.

[19] R. Farchioni, G. Grosso, „*Organic Electronic Materials“*, Springer Verlag Berlin Heidelberg, 2001, 182-183.

[20] Comitee on Polymer Science and Engineering (R.S. Stein, chair), *“Polymer Science and Engineering”,* National Academy Press, Washington D.C., 1994, 50-52.

[21] M. G. Mikhael, A. B. Padias, H. K. Hall jr., *J. Polym. Sci. Part A* **1997**, *35*, 1673.

[22] A. G. MacDiarmid, J. C. Chiang, M. Halpern, W. S. Huang, S. L. Mu, N. L. Somasiri, W. Wu and S. I. Yaniger, *Mol. Cryst. Liq. Cryst.* **1985**, *121*, 173.

[23] W. S. Huang, B. D. Humphrey and A. G. MacDiarmid, *J. Chem. Soc. Faraday Trans 1.* **1986**, *8*, 2385.

[24] G. G. Wallace, G. M. Spinks, L. A. P. Kane-Maguire, P. R. Teasdale, “*Conductive Electroactive Polymers”,* CRC Press LLC, Florida, 2nd ed, pp. 121-159, 2003.

[25] Ch. H. McCoy, I. M. Lorković, M. S. Wrighton, *J. Am. Chem. Soc.* **1995,** 117, 6934-6943.

[26] G. G. Wallace, G. M. Spinks, L. A. P. Kane-Maguire, P. R. Teasdale, “*Conductive Electroactive Polymers”,* CRC Press LLC, Florida, 2nd ed, pp. 161-177, 2003.

[27] D. Yang, P. N. Adams and B. R. Mattes, *Synth. Met.* **2001**, *119*, 301.

[28] G. G. Wallace, G. M. Spinks, L. A. P. Kane-Maguire, P. R. Teasdale, “*Conductive Electroactive Polymers”,* CRC Press LLC, Florida, 2nd ed, pp. 146-152, 2003.

[29] M. Angelopoulos, G. E. Asturias, S. P. Ermer, E. M. Scherr, A. G. MacDiarmid, M. Akhtar, Z. Kiss and A. J. Epstein, *Mol. Cryst. Liq. Cryst.* **1988**, *160*, 151.

[30] J. Tanaka, N. Mashita, J. Mizoguchi and K. Kume, *Synth. Meth.* **1989**, *29*, E175.

[31] D.-K. Moon, M. Ezuka, T. Maruyama, K. Osakada and T. Yamamoto, *Macromolecules* **1993**, *26*, 364.

[32] Y. Wei, R. Hariharan and S. A. Patel, *Macromolecules* **1990**, *23*, 758.

[33] D. MaCinnes Jr. and B. L. Funt, *Synth. Met.* **1988**, *25*, 235.

[34] Y. Wei, W. W. Focke, G. E. Wnek, A.Ray and A. G. MaDiarmid, *J. Phys. Chem.* **1989**, *22*, 3521.

[35] G. Venugopal, X. Quan, G.E. Johnson, F. M. Houlihan, E. Chin, O. Nalamasu, *Chem. Mater.* **1995**, *7*, 271.

[36] S. X. Cai, M. Kanskar, J. C. Nabity, J. F. W. Keana, M. N. Wybourne, *J. Vac. Sci. Technol. B* **1992**, *10*, 2589.

[37] D. M. de Leeuw, P. W. M. Blom, C. M. Hart, C. M. J.Mutsaers, C. J. Drury, M. Matters, H. Termeer, *IEDM Tech. Dig.* **1997**, 13.

[38] C. J. Drury, C. M. J. Mutsaers, C. M. Hart, M. Matters, D. M. de Leeuw, *Appl. Phys. Lett.* **1998** *73*, 108.

[39] C. W. Lee, Y. H. Seo, S. H. Lee, *Macromolecules* **2004**, *37*, 4070.

[40] M. Angelopoulos, N. Patel, J. M. Shaw, N. C. Labianca, S.A. Rishton, *J. Vac. Sci. Technol. B* **1993**, *11*, 2794.

[41] B. K. Barnet, T. D. J Roberts, *Chem Soc, Chem. Commun.* **1972**, 758.

[42] M. Shirai, M. Suzuki, T. Saito, M. Koyama, M. Tsunooka, *Makromol. Chem.* **1991**, *192*, 1447.

[43] T. Griesser, A. Wolfberger, M. Edler, M. Belzik, G. Jakopic, G. Trimmel, W. Kern, *J. Poly. Sci. A* **2010**, *48*, 3507.

[44] D.-K. Moon, M. Ezuka, T. Maruyama, K. Osakada, T. Yamamoto, *Makromol. Chem*. **1993**, *194*, 3149.

[45] C. B. Duke, E. M. Conwell, A. Paton *Chem. Phys. Lett.* **1986**, *131*, 82.

[46] S. Stafstrom, J. L. Bredas, A. J. Epstein, H. S. Woo, D. B. Tanner, W. S. Huang, A. G. MacDiarmid *Phys. Rev. Lett.* **1987**, *59*, 1464.

[47] Y. Yang, A. J. Heeger, *Appl. Phys. Lett.* **1994**, *64*, 1245.

[48] H. E. Gottlieb, V. Kotlyar, A. Nudelman, *J. Org. Chem.* **1997**, *62*, 7512.